Crustal structure of the Western Azuero Peninsula, Panama

Insights into the structure of accretionary complexes and forearc ophiolites

Ortiz-Guerrero, Carolina; Montes, Camilo; Farris, David W.; Agudelo, Catalina; Ariza Acero, Margarita; Ayala, Juliana; Avellaneda, Jose David; Cortes-Calderon, Alejandro; Revelo-Obando, Billy; More Authors

DOI
10.1080/00206814.2023.2191678

Publication date
2023

Document Version
Final published version

Published in
International Geology Review

International Geology Review

ISSN: (Print) (Online) Journal homepage: https://www.tandfonline.com/loi/tigr20

Crustal structure of the Western Azuero Peninsula, Panama: Insights into the structure of accretionary complexes and forearc ophiolites

Carolina Ortiz-Guerrero, Camilo Montes, David W. Farris, Catalina Agudelo, Margarita Ariza Acero, Juliana Ayala, Jose David Avellaneda, Alejandro Cortes-Calderon, Esteban Gaitan, Sebastian Garzon, Daniel Gongora-Blanco, Nubia Andrea Jara, Juan Camilo Meza-Cala, Lina Perez-Angel, Nathalia Pineda-Rodríguez, Alejandro Rodriguez-Parra, Billy Revelo-Obando, Carolina Rubiano, Elena Stiles, Maria Paz Urdaneta, Nicolas Zuluaga, Felipe Lamus, Federico Moreno & Aldo Rincon

To cite this article: Carolina Ortiz-Guerrero, Camilo Montes, David W. Farris, Catalina Agudelo, Margarita Ariza Acero, Juliana Ayala, Jose David Avellaneda, Alejandro Cortes-Calderon, Esteban Gaitan, Sebastian Garzon, Daniel Gongora-Blanco, Nubia Andrea Jara, Juan Camilo Meza-Cala, Lina Perez-Angel, Nathalia Pineda-Rodríguez, Alejandro Rodriguez-Parra, Billy Revelo-Obando, Carolina Rubiano, Elena Stiles, Maria Paz Urdaneta, Nicolas Zuluaga, Felipe Lamus, Federico Moreno & Aldo Rincon (2023): Crustal structure of the Western Azuero Peninsula, Panama: Insights into the structure of accretionary complexes and forearc ophiolites, International Geology Review, DOI: 10.1080/00206814.2023.2191678

To link to this article: https://doi.org/10.1080/00206814.2023.2191678

INTERNATIONAL GEOLOGY REVIEW
https://doi.org/10.1080/00206814.2023.2191678

Taylor & Francis
Taylor & Francis Group

Crustal structure of the Western Azuero Peninsula, Panama: Insights into the structure of accretionary complexes and forearc ophiolites

Carolina Ortiz-Guerrero[a], Camilo Montes[b], David W. Farris[c], Catalina Agudelo[d], Margarita Ariza Acero[e], Juliana Ayala[d], Jose David Avellaneda[d], Alejandro Cortes-Calderon[f], Esteban Gaitan[g], Sebastian Garzon[h], Daniel Gongora-Blanco[d], Nubia Andrea Jara[d], Juan Camilo Meza-Cala[i,q], Lina Perez-Angel[j], Nathalia Pineda-Rodríguez[k], Alejandro Rodriguez-Parra[l], Billy Revelo-Obando[m], Carolina Rubiano[d], Elena Stiles[n], Maria Paz Urdaneta[d], Nicolas Zuluaga[o], Felipe Lamus[b], Federico Moreno[p] and Aldo Rincon[b]

[a]Department of Geological Sciences, University of Florida, Gainesville-FL, US; [b]Departamento de Física y Geociencias, Universidad del Norte, Barranquilla-Colombia; [c]East Carolina University, Department of Geological Sciences, Greenville-NC, US; [d]Departamento de Geociencias, Universidad de los Andes, Bogotá, Colombia; [e]Institute of Earth Sciences, University of Lausanne, Lausanne, Switzerland; [f]Institute of geochemistry and Petrology, ETH Zürich, Zürich, Switzerland; [g]Biogéosciences, UMR CNRS 6282, Université de Bourgogne, Dijon, France; [h]Laboratory of Geo-information Science and Remote Sensing, Wageningen University and Research, Wageningen, The Netherlands; [i]Centre for Earth Evolution and Dynamics (CEED), University of Oslo, Oslo, Norway; [j]Department of Earth, Environmental, and Planetary Sciences, Institute at Brown for Environment and Society (IBES), Brown University, Providence, Rhode Island, US; [k]Departamento de Geociencias, Universidad Nacional de Colombia, Bogotá, Colombia; [l]Ministerio de Minas y Energía, Bogotá, Colombia; [m]Department of Geoscience and Engineering, Delft University of Technology, Delft, The Netherlands; [n]Department of Biology, University of Washington, Seattle, WA, USA; [o]Centre for Exploration Targeting, University of Western Australia, Crawley, WA, Australia; [p]Department of Geosciences, University of Arizona, Tucson-Arizona, (US); [q]Department of Geosciences, University of Oslo, Oslo, Norway

ABSTRACT

Detailed geologic mapping (639 field stations in ~700 km^2) and a ~50 km-long gravity survey (142 stations) in the western Azuero Peninsula revealed two faulted and folded slivers of oceanic crust attached to the trailing edge of the Caribbean Large Igneous Plateau (CLIP). Our new data, along with published geochronology, allowed us to reconstruct the Cretaceous forearc configuration of the trailing edge of the CLIP prior to seamount collision, ophiolite accretion, and whole-margin deformation. The ophiolite in western Azuero is composed of two tectonic slivers arranged in south-verging, imbricated thrust faults that stack a ~73 Ma pillow, flow, and picritic basalt and black chert, together with a ~ 89–93 Ma and older basalt flows and capping red chert sequences. Accretion of these slivers to form a supra-subduction zone ophiolite resulted from the middle Eocene collision and accretion of Galapagos seamounts against the trailing edge of the CLIP. Accreted seamounts are arranged in a north-verging antiformal stack duplex, and below the thrust sheets. Change in kinematics after fission of the Cocos-Nazca Plate during early Miocene times prompted the propagation of the Azuero-Sona fault zone flower structure, favouring the preservation of these slivers of oceanic crust.

ARTICLE HISTORY
Received 12 July 2022
Accepted 13 March 2023

KEYWORDS
Forearc ophiolite; subduction margins; accretionary margins; Panama

Introduction

Anywhere asperities exist on a subducting plate, interactions at the trench lead to a variety of structural and tectonic readjustments in the margin that include processes such as subduction erosion (Vannucchi *et al*. 2016), formation of frontal contractional structures in the upper plate (von Huene *et al*. 2004), or collision-related vertical-axis rotations (McCabe 1984; Wallace *et al*. 2005, 2009). If those asperities are large and buoyant enough to congest the subduction zone, the ensuing collision may cause their emplacement along the accretionary complex, and also the tectonic duplication and emplacement of forearc crust onto the arc, by far the most common type of ophiolite emplacement (Beccaluva *et al*. 2004; Stern *et al*. 2012). Oceanic crust fragments thus emplaced belong to a forearc crust that formed when the overriding plate was under extension in a supra-subduction zone (SSZ) setting, and may contain the record of subduction initiation (Whattam and Stern 2011), or instead represent oceanic crust generated during trench rollback prior to terminal continental collision (Dilek and Furnes 2009, 2014, 2019). SSZ forearcs may also contain older lithospheric fragments trapped prior to ophiolite emplacement (DeBari *et al*. 1999). Materials scrapped off the subducting slab during accretionary processes (Johnson *et al*. 1991; Boschman *et al*. 2021) belong in the accretionary complex and keep the record of the downgoing plate.

CONTACT Camilo Montes camilomontes@uninorte.edu.co Department of Physics and Geology, Universidad del Norte, Barranquilla, Colombia
Supplemental data for this article can be accessed online at https://doi.org/10.1080/00206814.2023.2191678.

Ophiolites can be discriminated according to their affinity, or lack thereof, to subduction processes during their formation (Dilek 2003; Dilek and Furnes 2014). Subduction-related ophiolites include those formed in the extended upper plate of subduction zones such as incipient arcs, back-arcs and forearcs. Subduction unrelated ophiolites, form along mid-ocean ridges, and have contrasting crustal profiles according to spreading velocity: thinner or nearly absent sheeted dike complexes in slow-spreading ridges, and thicker with well-developed ones in fast-spreading ridges. Plume-related ophiolites, also subduction un-related like the circum-Caribbean western Cordillera of Colombia, show thick massive lava flow sequences and intercalated metasediments, either accreted against (Kerr *et al*. 1998), or obducted on to the continental margin (Bourgois *et al*. 1982). Within the subduction-related, or SSZ ophiolites, Beccaluva *et al*. (2004), recognize two main types: Tethyan and Cordilleran. The former is characterized by a steepening slab dip and rollback, which causes plate decoupling and extension in the forearc, and results in ophiolitic sections with extensive development of sheeted dike complexes, boninites, and few differentiated magmatic products. When collision takes place, the forearc lithosphere gets displaced from its tectonic setting above the subduction zone, and is emplaced as a coherent supra-subduction zone ophiolite onto the margin. Cordilleran ophiolites are instead the result of steady-state subduction regimes (high velocity and constant slab dip), with greater differentiated magmatic products with time with respect to Tethyan ophiolites, and no sheeted dike complexes – at least not in circum-Caribbean ophiolites. In Cordilleran ophiolites, collision with buoyant asperities in the subducting plate usually emplaces dismembered forearc ophiolite slices (Stern *et al*. 2012) against the margin through accretionary processes, instead of as coherent, intact obducted crustal sections more common in Tethyan ophiolites (Beccaluva *et al*. 2004).

The Azuero Peninsula in Panama (Figure 1) has been interpreted as an example of the interaction between asperities (Galapagos-born seamounts, Hoernle *et al*. 2002; Buchs *et al*. 2011) in the down-going plate, and the intra-oceanic Central American arc (Wegner *et al*. 2011), built on top of the Caribbean Large Igneous Plateau (CLIP). While the accreted seamounts expose the stacked record of the Galapagos hotspot activity for the last 70 Ma (Hoernle *et al*. 2002; Gazel *et al*. 2018), the arc sequences allow the study of plume-induced (89–90 Ma, Sinton *et al*. 1998; Dürkefälden *et al*. 2019), subduction initiation processes (Whattam *et al*. 2020). A wide and rather heterogeneous age range of magmatic products is, however, present in the Azuero Peninsula with lavas as old as ~145 Ma (Figure 1 and SM1), at odds with a history of magmatic events starting at ~ 89–90 Ma. Surprisingly, however, and despite the intensity of sampling (Figure 1), no detailed geologic maps or cross-sections of the Azuero Peninsula

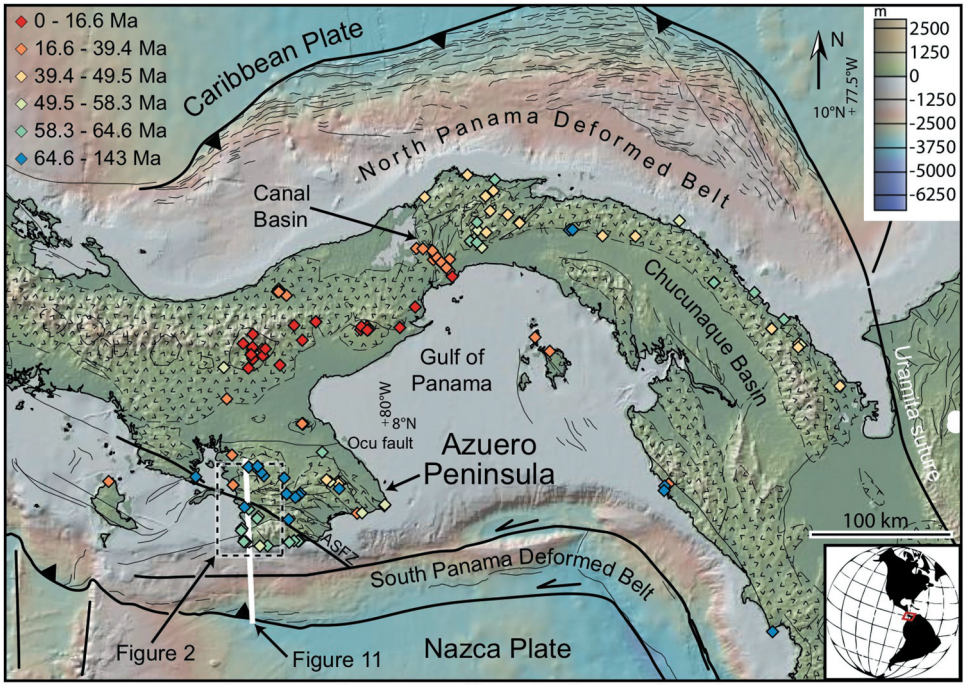

Figure 1. Regional setting of the Azuero Peninsula. Modified from Montes *et al*. (2012); bathymetry and shaded topography from Geomapapp. Ages of magmatic rocks (in pattern), coloured by age. See SM1 for compilation of ages and authors.

region exist, so these older sequences have not yet been fully characterized and investigated. The eastern, drier half of the Azuero Peninsula has been mapped in detail (Corral *et al*. 2013, 2016), though narrowly missing the arc-accretionary complex boundary. The United Nations mining project (Guidice and Recchi 1969) and the works by Buchs et al. (Buchs *et al*. 2010, 2011) have presented geologic maps of the western side of the peninsula, but only at small scales (~1:500.000).

In this contribution, we combine new detailed geological mapping performed at 1:24.000 scale, structural cross-sections, published geochronological data, and a ~50 km-long geophysical transect along the western Azuero Peninsula. Mapping in Azuero is facilitated by key markers such as limestone, black or red chert, pillow basalt, picrites, or peridotites within a dense drainage network, and km-long, wave-cut platforms where the thick tropical saprolite is absent and rock exposures can be continuous, or nearly so. Our approach here is relevant considering that the Azuero peninsula, as well as other supra-subduction zone ophiolites, have been studied mostly from a petrological and geochemical point of view, focusing in the emplacement and origin of lavas, without a complementary structural, or geophysical approach.

Geology of the Azuero Peninsula

In the following paragraphs, we summarize what is currently known about the basement and cover sequences in the Azuero Peninsula, including ages, affinities, and structure of the magmatic basement, as well as the thicknesses, composition and ages of the cover sequences, and the major structures that cross the peninsula.

Basement Composition

The Azuero Peninsula (Figure 1) is the westernmost exposed block of a Campanian to Eocene intraoceanic arc (Hoernle *et al*. 2004, 2008; Lissina 2005; Wegner *et al*. 2011; Montes *et al*. 2012, 2012), built on the trailing edge of the ~89–90 Ma (Sinton *et al*. 1998; Dürkefälden *et al*. 2019) thickened Caribbean oceanic plateau (Case *et al*. 1990; Pindell and Kennan 2009). Parts of this left-laterally segmented, oroclinally bent, intraoceanic arc (Montes *et al*. 2012), have been variably called the Chorotega-Choco block (Duque-Caro 1990), the Chagres-Bayano arc (Lissina 2005; Wegner *et al*. 2011), the Panama arc (Coates *et al*. 2004), the Panama-Choco arc (Redwood 2019), and the Azuero arc and proto-arc (Buchs *et al*. 2010, 2011). Regardless of nomenclature (see review in Montes and Hoyos 2020), this intraoceanic, segmented arc is composed of a fairly deformed basement complex made of basaltic flows and interbedded pelagic and hemipelagic sediments, intruded by Campanian to early Eocene intermediate plutonic rocks and mafic dikes.

In general, magmatic products in the Central American arc change from plume-contaminated (Whattam 2018; Whattam *et al*. 2020), MORB-like to volcanic arc-like with time (Lissina 2005; Wörner *et al*. 2009; Corral *et al*. 2011; Wegner *et al*. 2011). In this scenario, subduction initiation would have been prompted by a vigorous event of ~95–83 Ma plume-related volcanism (Sinton *et al*. 1998; Dürkefälden *et al*. 2019) that gave rise to the Caribbean Plateau. Younger plateau ages reported in the circum-Caribbean (Kerr *et al*. 1997; Revillon *et al*. 2000), may be disturbed ages, suffering from loss of ^{40}Ar subsequent to crystallization, due to magmatic, tectonic or hydrothermal events, consistent with a plateau older than ~ 86 Ma (Ariza-Acero *et al*. 2022).

Very shortly after the plateau was established, or perhaps simultaneously, a subduction-related magmatic arc developed along its trailing edge (Whattam *et al*. 2020). Detrital zircon geochronology of modern sands confirms the presence of 100–84 Ma (~90 Ma mean age), isotopically juvenile zircons with a typical subduction arc signature in the Isthmus of Panama (Leon *et al*. 2022). This modern sand dataset suggests that plateau (CLIP) extrusion was followed very shortly afterwards, or nearly simultaneously, by subduction initiation and arc magmatism at ~90 Ma, then by extrusion of forearc basalts in the Azuero-Sona at 75–73 Ma (Buchs *et al*. 2010), with primitive lavas (Mg# > 60), and later in the slightly younger Chagres-Bayano suites (Whattam *et al*. 2020). Therefore, magmatism and extension may have taken place after plateau extrusion and subduction initiation in a supra-subduction forearc setting.

Alternative hypothesis suggests that subduction initiation was forced by tectonic changes taking place simultaneously with cessation of vigorous plume activity at the Galapagos hotspot at ~71 Ma (Wegner *et al*. 2011), or perhaps a few million years earlier at ~75–73 Ma as the leading edge of the thickened Caribbean Plate collided with South America, and placed the plate under compression (Buchs *et al*. 2010). Continued subduction of the Farallon Plate beneath the CLIP would have produced a magmatic transition to early arc magmatism (75–70 Ma), emplacing submarine lavas flows in Panama and Costa Rica (Lissina 2005; Buchs *et al*. 2010; Wegner *et al*. 2011; Corral *et al*. 2013).

Separate from the Campanian to Eocene intraoceanic arc, the southwestern corner of the Azuero

peninsula contains the compressed history of the Galapagos hotspot, as seamounts spawned at the hotspot were sequentially transported to the Central American trench (Hoernle *et al*. 2002; Lissina 2005; Buchs *et al*. 2011), accreted in mid-Eocene times (Buchs *et al*. 2010), and later overlapped by upper Eocene and younger clastic strata (Kolarsky *et al*. 1995). After accretion of the Galapagos-derived seamounts, fission of the Farallon Plate took place in earliest Miocene times (Lonsdale and Klitgord 1978; Lonsdale 2005; McGirr *et al*. 2021), changing the margin in Azuero from subduction to predominantly left-lateral strike-slip (Westbrook *et al*. 1995).

Interbedded Limestone and Chert Units

The submarine basaltic successions of the Azuero peninsula basement are locally interbedded with hemi-pelagic limestone, mudstone, siltstone, and tuff. The hemipelagic limestones are light-grey, and characteristically bioturbated, dated as late Campanian to Maastrichtian using planktonic foraminifera (Fisher 1965; Guidice and Recchi 1969; Buchs *et al*. 2010; Corral *et al*. 2013). These carbonates include the Torio Limestone and Ocu Formation in the Azuero Peninsula and nearby Coiba island (Hershey 1901; Guidice and Recchi 1969; Kolarsky *et al*. 1995), the Changuinola Fm. in northwestern Panama (Fisher 1965), and the lower member of the Rio Quema Fm. in eastern Azuero Peninsula (Corral *et al*. 2016). The Rio Quema Formation in eastern Azuero consists of a ~1700 m-thick volcano sedimentary sequence representing the forearc of the Panama Cretaceous volcanic arc. The lower unit consists mostly of andesitic lava flows interbedded with turbidites, ash layers, and hemipelagic limestone and chert. The upper unit contains volcaniclastic sediments interbedded with andesitic lava flows, dacitic rocks and conglomerates (Corral *et al*. 2016). Geologic maps of Corral et al. (2011, 2013), locate the transition from plume to subduction-related volcanism using these hemipelagic units.

Older pelagic units include locally distorted red chert interlayered with, or in lenses within basalts in the Azuero Peninsula. Biostratigraphic analyses of a radiolarite sample in Torio Beach (Figure 2), indicate a Coniacian age (89–86 Ma, Kolarsky *et al*. 1995). In this context, two amphibole Ar/Ar step – heating plateau ages from the volcanoclastic rocks of the Rio Quema Formation (143 ± 11 Ma and 105 ± 3 Ma, Corral *et al*. 2016), could represent fragments of older lithosphere trapped within the arc basement (CLIP). Lissina (2005), similarly reports Ar/Ar ages of 93.5 ± 5.3 Ma in massive basalts near the Azuero-Sona fault zone (Figure 1, and SM1), and older ages of 114.5 ± 2 Ma in tholeiites eastern Azuero Peninsula that were interpreted as plateau rocks (the former), and the basement previous to the extrusion of the plateau (the latter).

Late Dikes

Metre-scale mafic dikes with plagioclase and clinopyroxene, recognized by most authors in the Azuero Peninsula, crosscut all igneous and volcanic basement sequences described up to this point. These undeformed mafic dikes are cutting metamorphic sequences with well-developed schistosity, so they effectively constrain the minimum age for a deformation episode that took place before intrusion of these dikes. Whole rock K/Ar dates (39.4 ± 2.7 Ma, Tournon and Bellon 2009) indicate that the main deformational episode, at least in western Azuero, predates the middle Eocene. This middle Eocene episode is consistent with the main episode that deformed the Campanian to Eocene arc in the eastern Panama Isthmus (Montes *et al*. 2012).

Accreted Seamounts

Along the southwestern corner of the Azuero Peninsula, Buchs *et al*. (2011) describe a series of basaltic lava flows interbedded with hemipelagic limestone, basaltic breccia, and subaerial basaltic lava. These sequences are intruded by gabbros and basaltic dikes along a rift zone, and interpreted to be separated from the autochthonous sequences to the northeast by the kilometre-thick Azuero Melange along the ASFZ. These sequences were interpreted as two accreted seamounts (Buchs *et al*. 2010).

Cover Sequences

Non-conformably on top of the basement sequences of the Isthmus, a lower Eocene and younger, mildly deformed sedimentary sequence constitutes a cover sequence with very heterogeneous successions of clastic, pelagic and carbonate strata, preserved into several basin compartments from east to west: the Atrato-Chucunaque Basin (Barat *et al*. 2014), the Canal Basin (Woodring 1957; Farris *et al*. 2017; Buchs *et al*. 2019), and the Tonosi Basin (Kolarsky *et al*. 1995). West of the Azuero Peninsula, the arc and its basement/cover are concealed under the Miocene and younger volcanic and volcanoclastic cover of the Central American volcanic arc. To the east, they are continuous in the Western Cordillera of Colombia (Kellogg and Vega 1995).

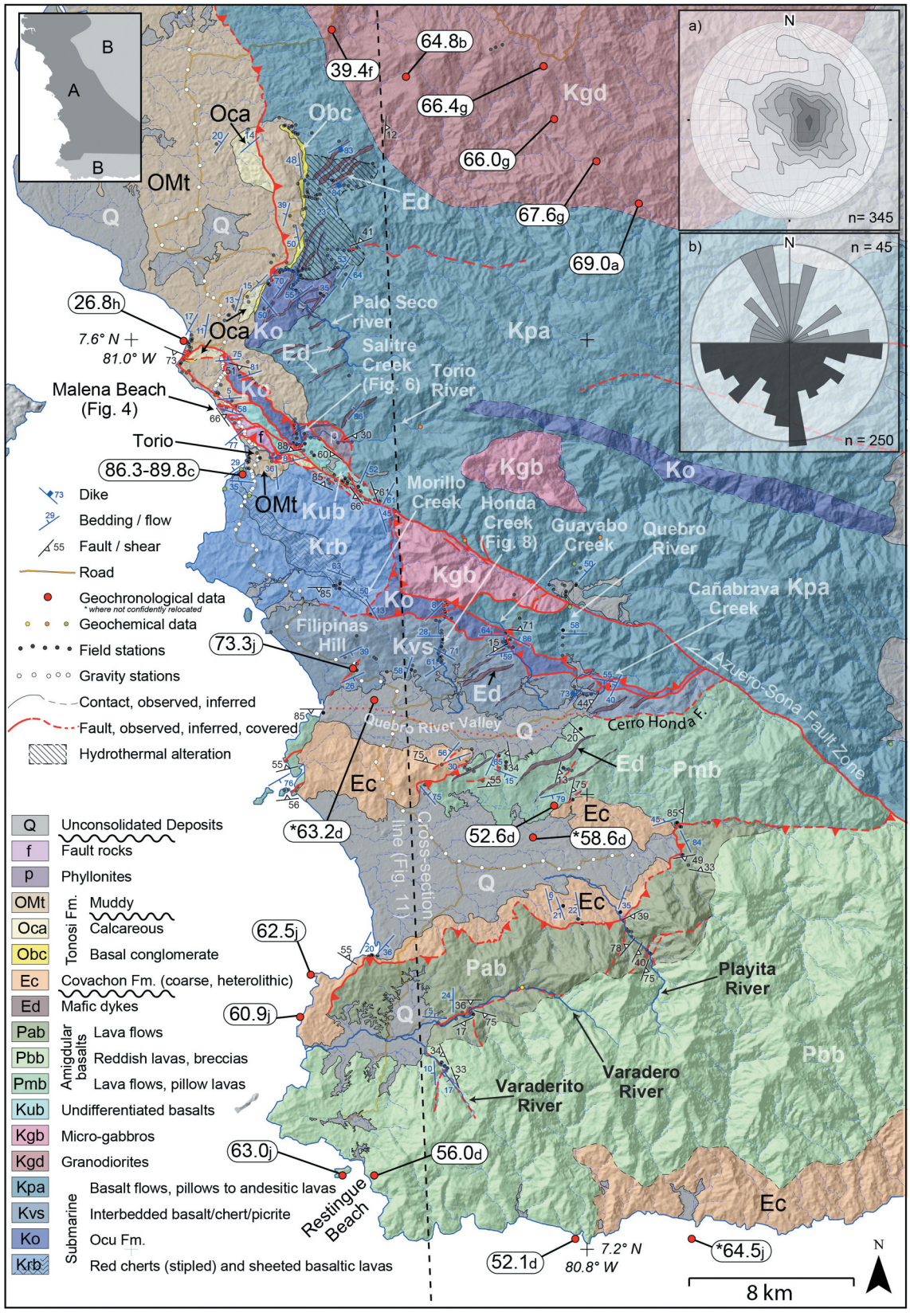

Figure 2. Geologic map of the western half of the Azuero Peninsula. Lower-hemisphere, equal-area projections plots of: A) kamb contours of poles to bedding (2 sigma contour interval), and B) dip direction of joints and dikes (top half-rose, 11% outer perimeter), and faults, foliation and cleavage (bottom half-rose, 8% outer perimeter), see SM2 for raw data. Geochronological ages in millions of years, subscripts indicate author (a: Guidice and Recchi 1969; b: Kesler *et al.* 1977; c: Kolarsky *et al.* 1995; d: Hoernle *et al.* 2002; e: Lissina 2005; f: Tournon and Bellon 2009; g: Montes *et al.* 2012; h: Kedenburg 2016; i: Ramirez *et al.* 2016 j: Gazel *et al.* 2018).

Autochthonous Cover Sequences

In the western half of the Azuero peninsula, the Tonosi Formation is a Cenozoic clastic/carbonate sedimentary sequence that has been mapped non-conformably overlying Upper Cretaceous and lower Eocene basement units. In Punta Malena, the Tonosi Formation was originally defined by Kolarsky *et al*. (1995), as a 1500-m-thick stratigraphic unit with two parts: a lower coarse-grained, and an upper, finer-grained segment. The lower unit is made of ~680 m of a massive, thickly bedded, basal conglomerate with planar bedding and coarsening upward cycles near the middle, and fining upward ones towards the top of the unit. This section was reported as barren of nannofossils, but in an equivalent section along the Palo Seco River (Figure 2), a palynological assemblage indicates an age younger than 33.7 Ma (Perez-Consuegra *et al*. 2018), that together with a zircon U-Pb age in a tuff near the top of this sequence (25.1 ± 0.18 Ma and 26.8 ± 2.2, Kedenburg 2016), suggest a mostly Oligocene age of accumulation, that may have started as early as late Eocene times (Buchs *et al*. 2011). A 432 m-thick, fine-grained, coarsening-upward shale-sandstone succession constitutes the Upper Tonosi Formation in Punta Malena (Kolarsky *et al*. 1995). The base of this fine-grained succession is marked by a calcarenite locally in faulted contact with the coarser-grained lower unit. Calcareous nannofossils indicate a late Oligocene to early Miocene time of accumulation (Kolarsky *et al*. 1995), an age range that overlaps nannofossil and palynological ages of a 50 m-thick unit, non-conformably resting on Coniacian red chert and basalt basement sequences in Torio Beach (Perez-Consuegra *et al*. 2018).

Both segments of the Tonosi Formation contain abundant well-preserved fossil fruits (Herrera *et al*. 2012; Perez-Consuegra *et al*. 2018), and mafic detrital components (Krawinkel *et al*. 1999), that suggest that the arc and its basement were already subaerial and eroding by the time of accumulation of these units.

Allochthonous Cover Sequences

An informal unit, the Covachon Fm., is a ~300-m-thick, shallowing-upward, locally chaotic, volcanoclastic unit deposited during early to middle Eocene times (Buchs *et al*. 2011), as aprons on Palaeocene to Eocene seamounts (Lissina 2005). Palaeocene ages (Gazel *et al*. 2018) reported on basalts within the mapped outcrop patterns of the Covachon Fm. (Figure 2), could correspond to large basaltic blocks within the more chaotic facies, lava flows within the unit, or unrecognized fault slices. Young ages (20.8 ± 1.8 Ma, Hoernle *et al*. 2002) reported in southern Azuero's Restingue Beach (Figure 2) deserve further scrutiny, as their stratigraphic position is seemingly above strata overlying unmapped Tonosi or Covachon formations. As noted by Lissina (2005), these young ages, as well as other similarly young ages in southern Azuero (32.1 and 16.6 Ma, Lissina 2005), all have small plateaus, and we therefore exclude them from further analysis (see SM1 for full table and details).

The coarse, chaotic cover sequences in the Azuero Peninsula have been interpreted to record outer forearc growth by underplating and subsequent erosion of accreted seamount volcanoclastic aprons, while the finer-grained, upper unit records upper Eocene to lower Miocene turbiditic flows as the forearc subsided and thinned, following subduction erosion (Krawinkel *et al*. 1999; Buchs *et al*. 2011).

The Azuero-Sona Fault Zone

The Azuero Peninsula hosts a sharp, prominent structural lineament defined as the Azuero-Sona Fault Zone (ASFZ). Mann and Corrigan (1990) described the ASFZ as a 1–2 km wide, sinistral shear zone, striking N64°W, that crosscuts all the Cretaceous and Cenozoic sequences (Figure 2), and develops a bold topographic lineament suggestive of Neogene to recent tectonic activity (Rockwell *et al*. 2010). Fabric elements within the fault zone include a sliver of fault-related, foliated mafic metamorphic rocks (Guidice and Recchi 1969; Tournon *et al*. 1989).

Previous studies place the boundary between the accreted seamounts and the Central American arc along the Azuero Melange, a swath of blocks and lenses of diverse origins tens to hundreds of metres thick, bound to the north by the ASFZ (Buchs *et al*. 2011, 2011). Further, the Azuero Melange was correlated to the Osa Melange, ~250 km to the west in the Osa Peninsula of Costa Rica, which Vannucchi *et al*. (2007) interpret as the result of tectonic shearing of subducting oceanic crust exotic to the upper plate margin, followed by underplating at depth. A Coniacian red chert

Geochemical data from Buchs *et al*. (2010), yellow: proto-arc; orange: arc; green: plateau affinities. Upper left inset shows areas of original mapping (A), and areas compiled from published maps (B: Guidice and Recchi 1969; Mann and Corrigan 1990; Kolarsky *et al*. 1995; MICI 1996; Buchs *et al*. 2010, 2011; Corral *et al*. 2011, 2013, 2017). Age of units is indicated by the uppercase letter in their code: K: Cretaceous; P: Paleocene; E: Eocene; O: Oligocene; M: Miocene.

conformably interlayered with basalt flows, south of the ASFZ (Kolarsky *et al*. 1995) seems, however, incompatible with the role of the ASFZ as the boundary between the Coniacian plateau and the Palaeocene seamounts (Hoernle *et al*. 2002; Gazel *et al*. 2018).

Palaeomagnetic data in the Azuero Peninsula (Di Marco *et al*. 1995; Rodriguez-Parra *et al*. 2017) show two distinct clusters not separated by the ASFZ, but instead by the Cerro Honda Fault (Figure 2). The northern domain, that includes localities south of the ASFZ, has consistent large clockwise vertical-axis rotations, with similar inclination and declination values. The southern domain instead presents scattered inclination/declination values consistent with the collision and dismemberment of far-travelled seamounts carrying different palaeomagnetic components (e.g. McCabe 1984). In summary, both palaeomagnetic data and reports of Coniacian radiolarites in the southern block of the ASFZ, suggest that the suture with accreted seamounts is located further south.

Methodology

Mapping

Two field seasons were completed in the southwestern Azuero Peninsula, covering an area of ~700 km^2, where geological and gravity data were measured. Traditional geologic mapping tracing contacts in the field, was carried out at a scale 1:24,000 mostly along creek beds, and low-tide, km-long, wave-cut platforms, and to a much lesser degree, road cuts. Observations and sampling took place nearly exclusively along creek beds, and wave-cut platforms to ensure fresh samples. A total of 639 field stations with structural, and lithological descriptions were georeferenced with hand-held GPS devices using dip, and dip-direction in azimuth (see SM2). Collection of structural and strain data was focused in 4 localities: Malena Beach, Torio, Salitre and Honda creeks, with additional transects along the Palo Seco, Torio, Playita, Varadero and Varaderito rivers (Figure 2). Thin sections were prepared on selected specimens (SM4). The structural profiles presented in this study were measured using measuring tape and compass, and registered to the geological mapping. Structural data were corrected and projected over generated topography with a linear nomogram method (Compton 1985) for cross-section construction.

Gravity data Collection and Processing

A total of 142 gravimetry stations were measured, with offsets of ~1 km in localities far from the mapped trace of the ASFZ, and 200–300 m in localities closer to the fault. Gravity measurements were collected using a Worden gravimeter with a zero-length quartz spring. The instrument has a precision of 0.01 mGal and a measurement reproducibility of 0.1–0.3 mGal over multi-year periods. A Trimble ProXRT differential GPS was used to locate gravity stations with an average elevation precision of 0.41 ± 0.13 m. All data in the survey was tied to a locally established base station in Torio at which repeat measurements were taken every day (7 am and 5 pm) to account for instrument drift and Earth tides. The local base station in Torio was tied to an absolute gravity measurement at the Instituto Geografico Nacional Tommy Guardia, in Panama City of 978,226.963 mGal (Panama City INGTG, D'agostino *et al*. 2010). Data collected in the field were corrected for drift, tides, elevation and local topography to derive the free-air and Bouguer anomalies. Terrane corrections were calculated out to 30 km using a 90 m SRTM digital elevation model and have values between 0.07 and 0.18 mGal. All elevations were measured and calculated using the EGM96 geoid vertical datum. Bouguer corrections used a reduction density of 2675 kg/m^3, and a gravitational constant G of 6.6743 × 10–11 Nm^2/kg^2. Overall, total precision and reproducibility of the gravity measurements is estimated at approximately 0.3 mGal.

Results

The geologic map (Figures 2 and 3) shows three main tectono-stratigraphic domains: 1) a northern domain north of the ASFZ, generally characterized by folded basalt sequences interbedded with hemipelagic limestones (Kpa and Kpo in Figure 2), and intruded by granodioritic to gabbroic bodies (Kgb and Kgd); 2) a southern domain south of the Cerro Honda Fault, characterized by vesicular and pillow basalts and coarse volcanoclastic sequences (Pab, Pbb and Pmb); and 3) a central domain between the ASFZ and the Cerro Honda Fault, with a folded and faulted belt of coherent, mappable, mafic to ultramafic rocks with interbedded cherts (Krb and Kvs), as well as other lithologic types also found in the northern domain (Ko, Kgb and Kpa).

In the following paragraphs, we highlight three field transects; first, the faulted/folded sequences of the ASFZ along Malena Beach, second, the folded/faulted carbonates in the Salitre Creek, and finally, the thrust sheets in the hanging wall of Cerro Honda Fault, along the Honda Creek. These sections are of crucial importance in the mapping and structural sections because they reveal key cross-cutting relationships and help define the structural style of the western Azuero Peninsula.

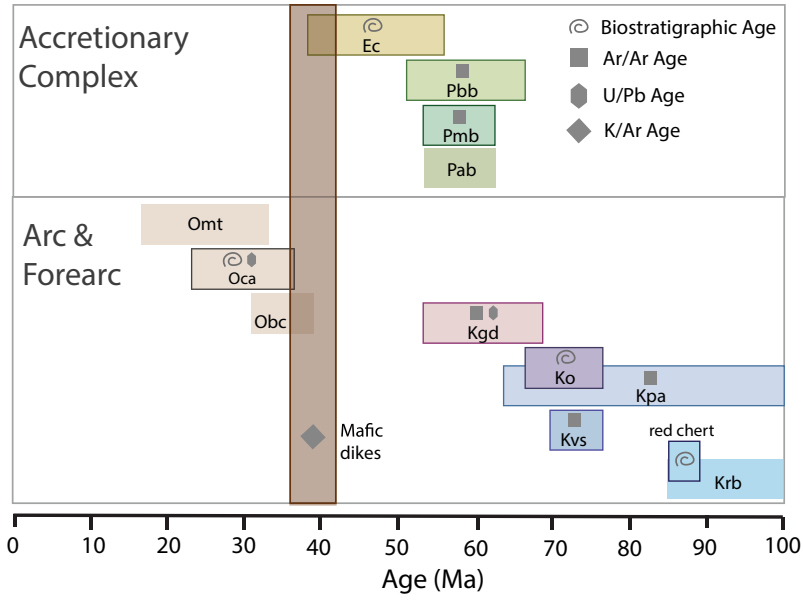

Figure 3. Chronostratigraphic chart showing the distribution of lithostratigraphic units in the western part of the Azuero Peninsula. All unit keys and colours as in Figure 2. Symbols represent the kind of geochronologic control for each unit.

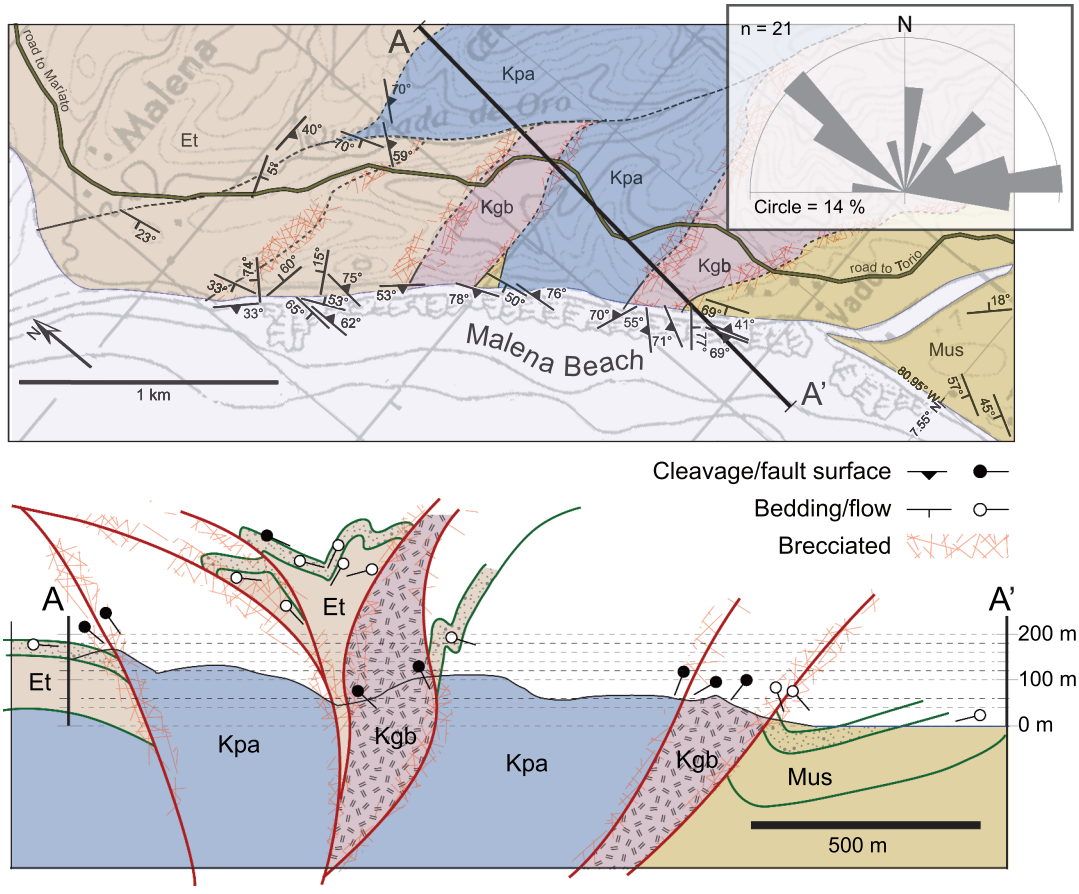

Figure 4. Geologic map and cross-section of the ASFZ in Malena Beach. Down-plunge projection of map data allows reconstruction of structures. Inset shows a half-rose diagram showing the dip direction of cleavage and fault planes. Note that roadcuts in western Azuero offer virtually no outcrops to control mapping. See Fig. 2 for location and labels of rock types.

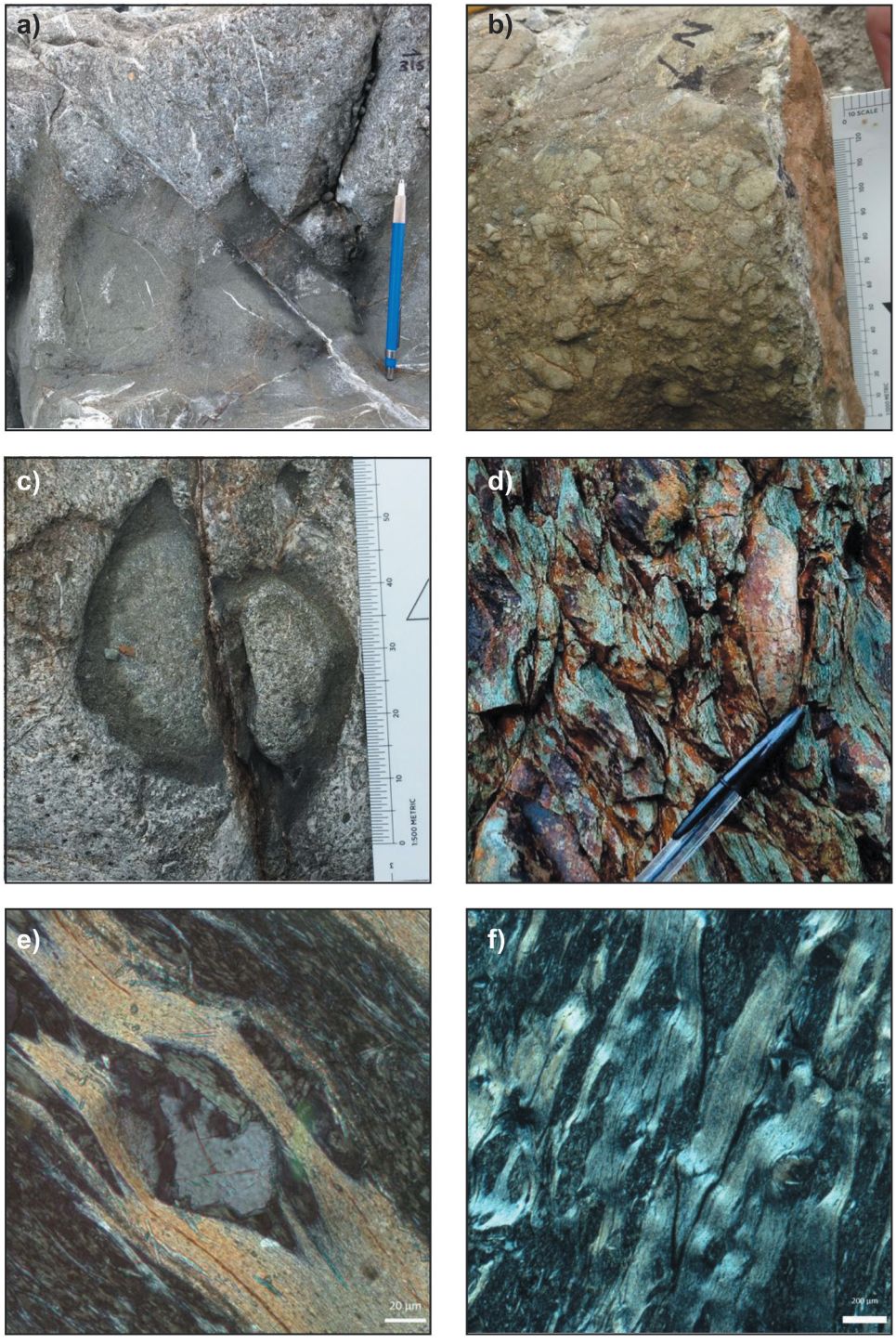

Figure 5. Outcrop photos of deformation fabrics in the Azuero-Sona Fault Zone. A) domino-style northwest-dipping faults in sandstone/wackstone sequence; B) fault breccia from a carbonate protolith; C) mafic clast in wackstone-matrix conglomerate with dextral sense of shear; D) phyllonite showing prominent rough S-C foliation and sigmoidal lenses with fresh basaltic cores at Torio Creek. Photomicrographs of ultramafic mylonite (sample # 38639) at Torio creek: E) diopside porphyroclast under cross-polarized light, showing dextral sense of shear and flow texture; F) augen-like texture showing kink-bands of chlorite+actinolite.

Malena Beach

At Malena Beach (Figure 2), a nearly continuous, albeit very oblique, ~ 2 km section of the ASFZ can be studied during low tide (Figure 4). Here, the vertical cliffs and wave-cut platforms show a succession of coherent, hundred-metre long blocks of sandy and conglomeratic limestone, sandstone, basalt, chert, and gabbro separated by discrete brittle faults roughly trending north

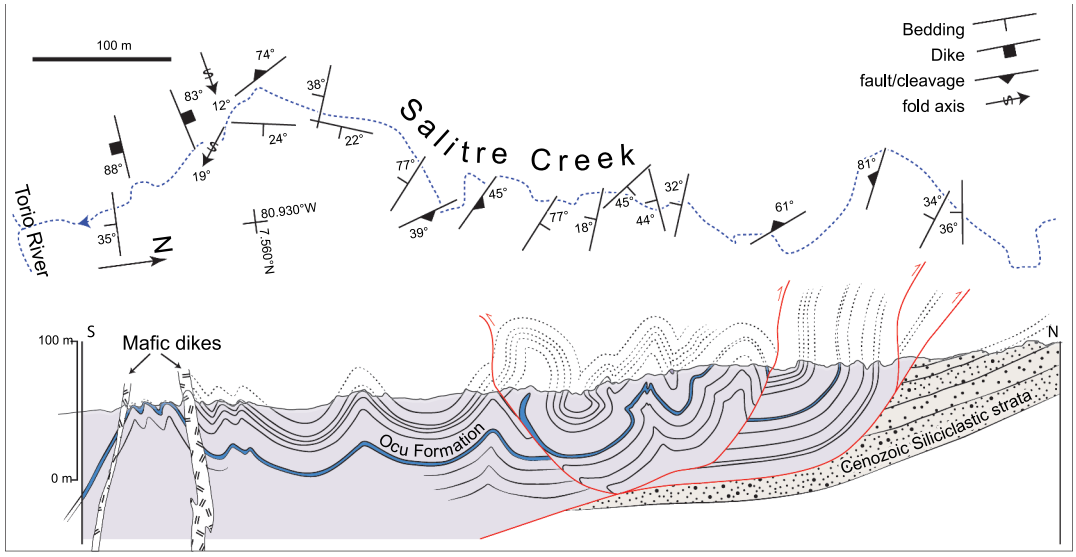

Figure 6. Map and cross-section along the Salitre Creek showing a folded, north-verging thrust sheet carrying a segment of the calcareous Ocu Fm. on top of Cenozoic strata of the Tonosi Fm. To the south, this sheet is faulted against basalts and phyllonites along the ASFZ. See Fig. 2 for location.

and northeast. Although the blocks are internally faulted and deformed, they remain recognizable (Figure 5a-c), with gouge, cataclasite and fault breccia occasionally 50 m-thick near the contacts with neighbouring blocks. Kinematic markers are ambiguous, showing both sinistral and dextral indicators.

Salitre Creek

Along Salitre Creek, the well-bedded nature of the Ocu Formation limestone reveals the intensity and style of deformation, as well as crucial cross-cutting relationships in this part of the peninsula (Figure 6). The Salitre Creek crosses a northwest-trending, lens-shaped, ~8 km long body of folded limestone in fault contact with mafic phyllonite (Figure 5d-f), and undifferentiated basalt. The hemipelagic limestone beds are correlatable to the Ocu Fm., with characteristically light-coloured, well bedded, and densely bioturbated limestone (Figure 7b-f), but lacking the typical basalt interbeds (Figure 7a), as probably only a small part of the sequence is repeated by folding.

From south to north, the creek exposes folded strata in mesoscopic open, cylindrical folds with shallow plunges. Folding intensity increases upstream, where box folds, tight, upright folds, with curved hinges in map view become common. Faults are marked by conspicuous brecciated limestone. The northern end of the section is marked by a north-verging thrust fault placing the folded carbonate sequence on top of a south-dipping, coarse-grained, well bedded, siliciclastic unit correlative to the Tonosi Fm. To the south of the section, mafic dikes intrude the folded sequence, and seem to post-date the main deformation episode, but they are not completely pristine or devoid of deformation. East of the mouth of the Salitre Creek with the Torio River, phyllonite with silky talc surfaces, basalt cores, and northwest-trending sigmoidal-shaped foliation is well exposed (Figure 5d), and grades to slightly sheared vesicular basalt and pillow basalts cross-cut by mafic dikes. Some of the outcrops appear to be hydrothermally altered, and shear sense indicators have recrystallized talc in the strain shadows or tails (Figure 5f).

La Honda Creek

A south-verging, faulted and folded sequence south from ASFZ, is composed of mafic rocks and black siliceous mudstones and cherts in La Honda Creek (Figure 8). A similar sequence is also present along-strike in the Cañabrava, and Guayabo creeks to the east (Figure 2), where medium-to-coarse grained picritic lava flows are found interbedded with vesicular basalts, pillow lavas, and black chert. The general trend of the faults is E-W, and their dip is commonly moderate to steep. Localized serpentinization and sigmoidal fault breccia within the volcanic rocks mark fault traces (Figure 9d). Lithologic types in the lower-southern part of the creek include coarse olivine-picritic lava flows (2–3 m thick), vesicular and pillowed basalt (also in nearly tabular 2–3 m flows), chert, black laminated mudstone, and volcanic breccia. The lower part of this sequence is cross-cut by diabase and basaltic dikes striking east. In the middle third of the creek, pillowed basalt (Figure 9c) is observed folded in open synform folds. Higher in the upper reaches of the

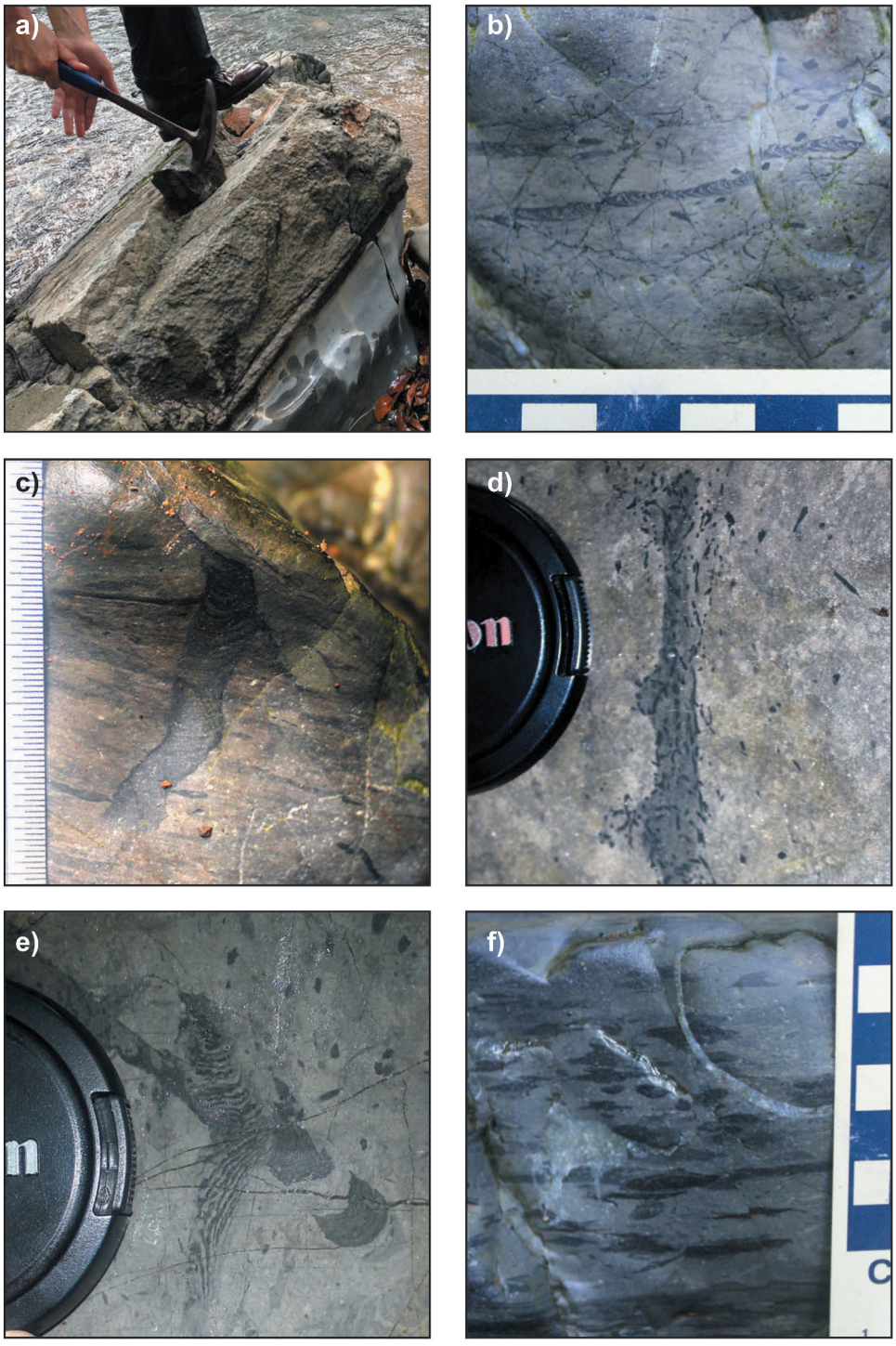

Figure 7. Field photos of Ocu Formation. A) Interbedded limestone and vesicular basalt flow, Palo Seco River; B. Sub-horizontal parallel spreiten structures, C. Vertical to sub-vertical burrow cross-cutting lenticular bedding, D. Sub-vertical burrow lined by mud pellets, E. Oblique view of likely horizontal to sub-horizontal spreite structures, F. Lateral view of discontinuous, likely bioturbated bedding, and 2-3 mm wide sub-horizontal to sub-vertical burrows infilled with lighter coloured sediment (see left of C on scale).

creek, thrust faults become steeper, and lava flows are interbedded with pillow lavas, and vesicular as well as non-vesicular basalts. Its upper contact towards the northern end of the section is faulted against a foliated, fine-grained gabbro with an intervening folded bioturbated limestone, chert and tuff from the Ocu Fm. West of the La Honda Creek section, and likely in a basal position, a sliver of massive ultramafic crystalline, serpentinized peridotitic body composed of serpentinized olivine and clinopyroxene (Figure 9e-F) crops out in Filipinas

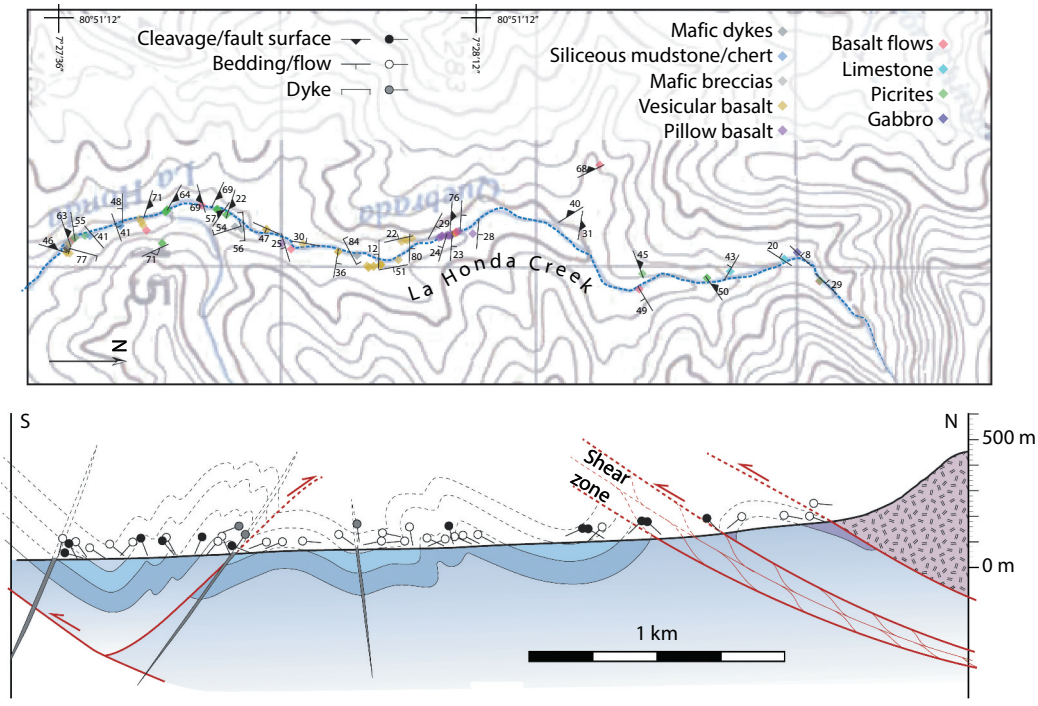

Figure 8. Map and cross-section along the Honda Creek showing the structure revealed by basalt flows, often picritic, and conformably interbedded chert and siliceous mudstone. This section represents the boundary between the plateau to the north, and the accreted seamount provinces to the south. See Fig. 2 for location.

Hill (Figure 2). Above these sequences, a red chert-bearing (Kolarsky *et al*. 1995), fault-bound, mappable (~8 km along the strike) basaltic unit crops out to the north (Krb in Figure 2). This unit is well exposed along the Morillo Creek (Figure 3a), and also in the southwestern corner of Torio Beach (Figure 9b). It is characterized by mesoscopic, conformable intercalations of red chert and basalts, well-bedded and coherent, along Morillo creek, and distorted, sometimes chaotic in Torio Beach as also noted by Kolarsky *et al*. (1995), and Lissina (2005).

Geologic Map

Because all the arc, proto-arc, plateau, and seamounts contain mostly basalt, we used interbedded key markers to discriminate and map five lithostratigraphic units (Figures 2 and 3). The first interbedded unit (Krb in Figure 2) is characterized by locally distorted, red chert beds and associated basalt flows (Figure 9a,b) Coniacian in age (Figure 2 near Torio). The second unit (Ko in Figure 2) is characterized by light grey, well-bedded, plane-parallel, bioturbated limestone beds (Figure 7b-f) intercalated with plane-parallel basalt flows (Figure 7a), pillow basalts, and greenish fine-grained tuffs; occasional plane-parallel black mudstone beds may also be present. It is well exposed in the Palo Seco River and the Salitre Creek, and its age is Campanian to Maastrichtian (Figures 2, 3). The third sequence well exposed in the Honda Creek (Kvs in Figure 2) is made of intercalated black chert and mudstone, crystal-rich picrite (Figure 9e), pillow lava (Figure 9c) and vesicular basalt with a peridotitic sole near Filipinas Hill (Figure 2), yielding Ar/Ar ages of ~73 Ma (Gazel *et al*. 2018). The fourth unit (Pab, Pmb, and Pbb in Figure 2) is characterized by thickly bedded volcanoclastic breccias, and mafic tuffs, all coarsely bedded, angular, and poorly sorted, interbedded with vesicular and pillow basalts with Palaeocene to early Eocene Ar/Ar ages (Figures 2 and 3; Hoernle *et al*. 2002; Gazel *et al*. 2018). The last unit is characterized by mostly clastic strata, which can be separated in two distinct units, one very coarse, volcanic and volcanoclastic (Ec in Figure 2), the other mostly well-bedded black mudstones (Obc, Oca, and OMt in Figure 2), both covering non-conformably underlying sequences, but involved in deformation, yielding biostratigraphic and geochronological ages from Oligocene to early Miocene (Kolarsky *et al*. 1995; Buchs *et al*. 2011; Kedenburg 2016; Perez-Consuegra *et al*. 2018).

In general, the geologic map shows that to the north, deformation is more pervasive, south-verging, while to the south, deformation structures are brittle, north-verging, and generally non-pervasive in volcanic and volcanoclastic rocks. All of the sequences above described are modified by shearing (Figure 5) both in

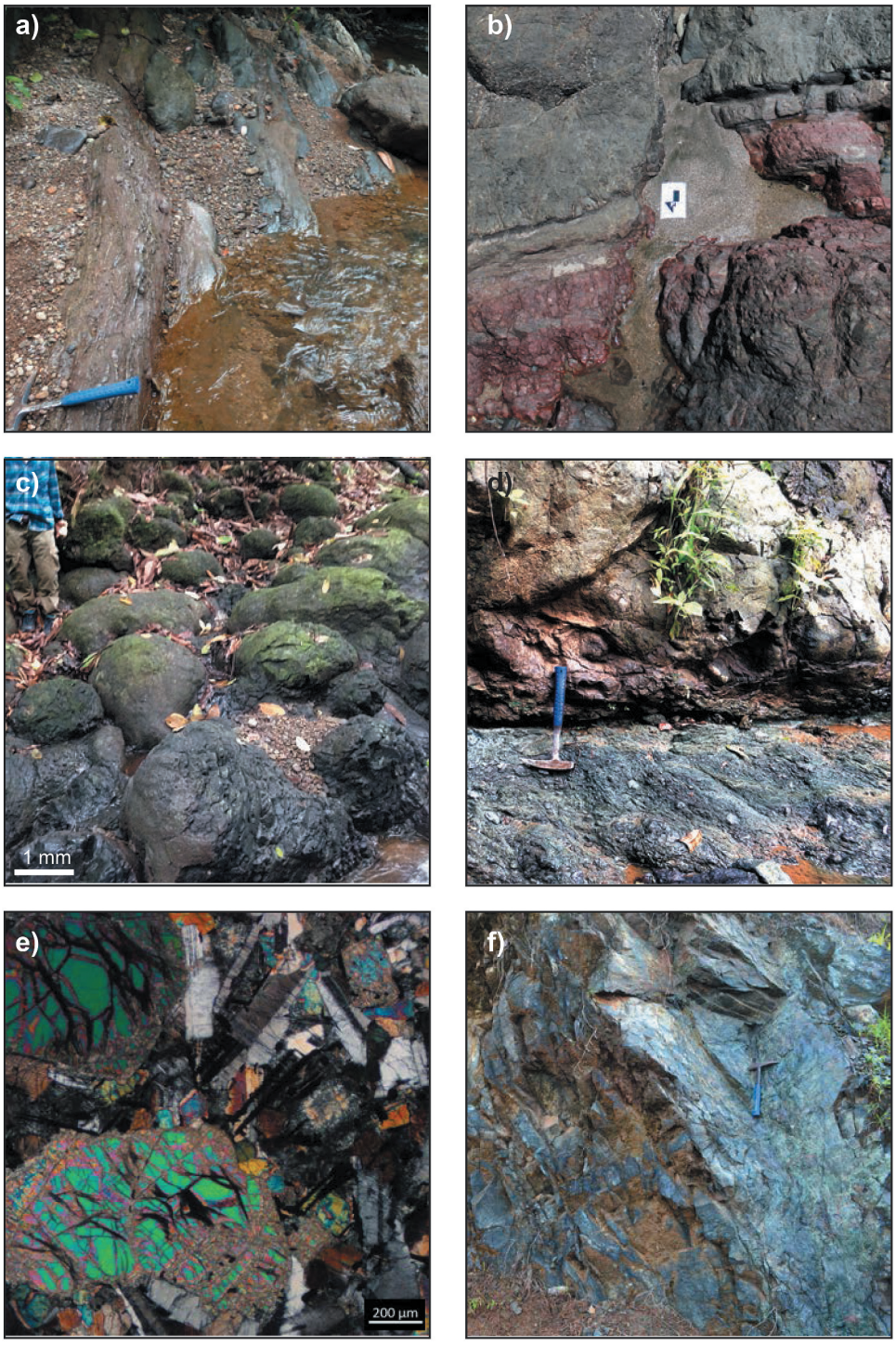

Figure 9. Field photos of: A) conformable succession of red cherts and basalts in Morillo Creek, and in B) Torio Beach; C) dipping pillow basalt sequence in Honda Creek; D) south-verging (left), sigmoidal shear zone in Cañabrava Creek; E) phaneritic texture in ultramafic sample 38,722 with abundant subhedral olivine (~50%), euhedral clino pyroxenes (~10%) and tabular plagioclase phenocrystals (~35%) in a serpentinized and chloritized matrix. F) massive aspect of the serpentinized peridotite in Filipinas Hill.

the brittle (f in Figure 2), and ductile domain (p in Figure 2), where breccias, cataclasites and mylonites develop mostly within the ASFZ, but also along other shear zones most notably those along the lower reaches of the Honda, Guayabo and Cañabrava creeks. A weakly deformed, northeast-trending, nearly vertical, mafic dike swath (Ed in Figure 2) cross-cuts all units except the cover sequences (Covachon and Tonosi Fms.); dike thickness varies from 1–5 metres, ranging from basalt to diabase. In general, the dikes tend to be notoriously

less fractured, deformed, or altered than their host rocks. The mapped pattern of the swath of northeast-striking dikes is left-laterally separated approximately 17 km across the ASFZ (Figure 2).

We correlate the first lithostratigraphic unit (Krb in Figure 2) with the Azuero Plateau because of the Coniacian age of the intercalated red cherts (Kolarsky *et al*. 1995) falls within the time of plateau extrusion (~89–90 Ma, Sinton *et al*. 1998; Dürkefälden *et al*. 2019). Also, three basalt samples south of Torio, within the Krb unit (Figure 2), have trace element contents suggestive of plateau geochemistry (Buchs *et al*. 2010). The second lithostratigraphic unit (Ko) can be correlated to the Ocu (Hershey 1901; Buchs *et al*. 2010) and Rio Quema (Corral *et al*. 2016) formations because of the distinctive light grey, bioturbated limestone successions intercalated with basaltic flows. The third lithostratigraphic sequence (Kvs) could not be correlated to any unit in the literature, although the Stack I unit of Buchs *et al*. (2011), bears similarities, but significantly, lacks calcareous sediments. An Ar/Ar age in a sample described as a picritic lava that yielded a 73.3 Ma age (Gazel *et al*. 2018) within this lithostratigraphic sequence. The fourth lithostratigraphic unit (Pab, Pmb, and Pbb) has extensive Palaeocene and early Eocene ages, and mostly falls within the seamount domain of Buchs *et al*. (2010). Finally, we correlate the fifth lithostratigraphic unit to the Covachon (Ec), and Tonosi (Obc, Oca and Omt), formations based on lithological similarities, geochronology (Kedenburg 2016) and micropalaeontological data (Perez-Consuegra *et al*. 2018).

Azuero-Sona Fault Zone Gravity Model

The gravity profile follows the main access road along the western edge of the Azuero Peninsula (Figure 2). The simple Bouguer anomaly (Figure 10) is nearly flat in the north with 60 to 70 mGal values, has a ~10 km segment where it gradually increases to ~ 80 mGal, and then progressively climbs towards the south to reach its maximum values at the southern end of the gravity transect, with 160 mGal, far larger than previous estimates for that region (Kellogg and Vega 1995; Mickus 2003). Corrections for drift, tides, latitude and elevation helped remove all the other factors that change gravity in the subsurface, leaving just the density factor.

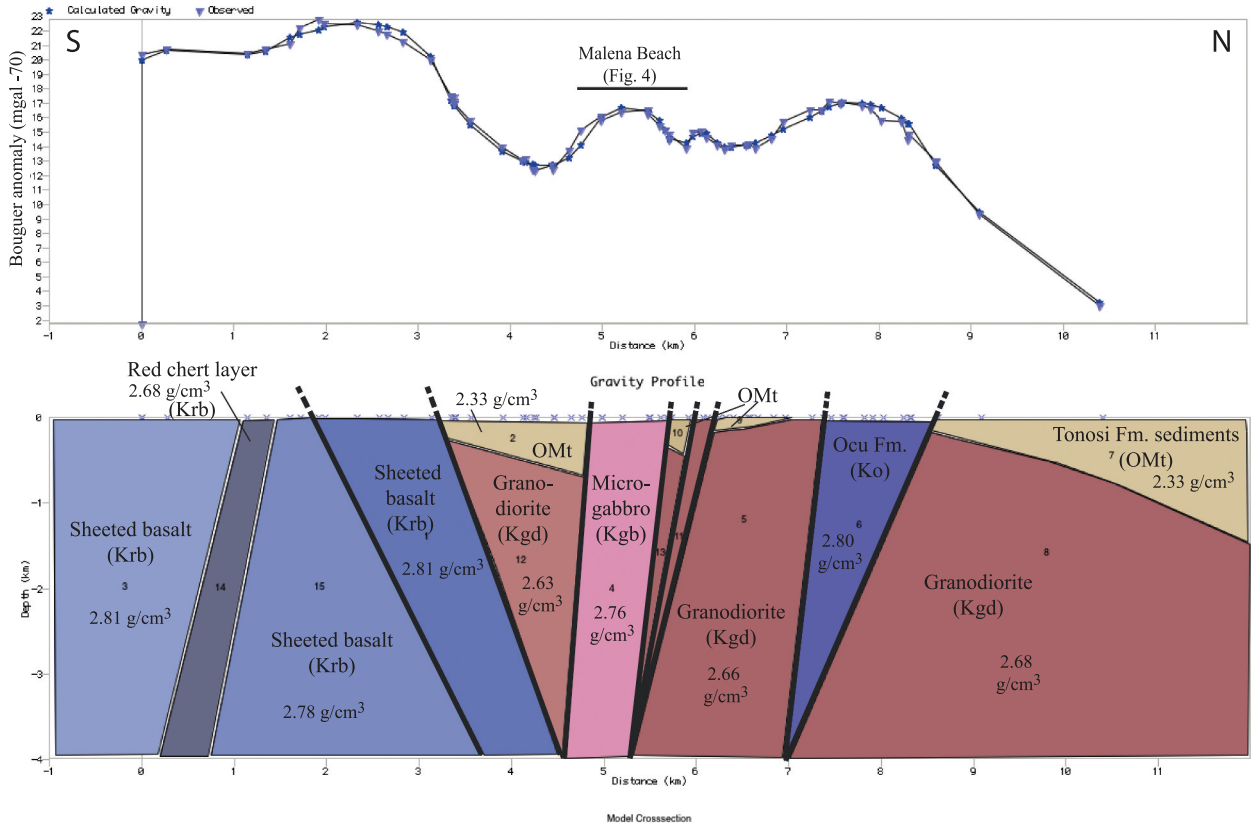

Figure 10. Gravity model of the Sona Azuero fault zone (ASFZ) showing a broad flower structure with outward radiating thrusts. This is a 2-D polygon-based gravity model constrained by surface geology and local density measurements. The ASFZ separates crustal blocks with higher density basaltic crust to the south from lower density granitic basement to the north. 70 mgal has been subtracted from Bouguer anomaly values so that upper crustal structure is more easily shown.

The gravity model (Figure 10) is a 2-D polygon-based model created using the GRAVMAG software (Burger *et al*. 2006) based on the method of Talwani *et al*. (1959). An assumption of 2-D models is that the individual blocks extend infinitely in and out of the plane. This assumption is approximately met by geologic units, such as those surrounding the ASFZ, that extend significantly along strike. The density of individual crustal blocks are constrained by density measurements throughout the Azuero Peninsula (See SM3), however there is a range of possible values for each block and density measurements are from the surface and not at depth. For example, Tonosi Fm. sediments range from 2.11 to 2.44 g/cm^3, and the 2.33 g/cm^3 used in the model is an estimate that takes into account sediments (dominantly sandstone) becoming more dense at depth. Similarly, basalt density measurements ranged from 2.75 to 3.13 g/cm^3. Values around 2.81 g/cm^3 were used in basalt dominated blocks to account for observations such as vesicle-rich layers and sedimentary interbeds.

Across the Azuero-Sona fault zone (ASFZ), higher spatial resolution gravity measurements were collected every 0.2–0.3 km over a transect approximately 9 km wide. This has allowed a detailed gravity model, constrained by surface geology and density measurements, to be constructed (Figure 10). The basic geology implied by the model is a large-scale flower structure centred on the ASFZ, and composed of kilometre-scale fragments of rocks from along the fault. Basement rocks north of the fault are largely granodioritic to dioritic in nature, whereas basement rocks south of the ASFZ are higher density and largely basaltic. In addition, the Tonosi Fm. basin forms a large, > 15 mGal, gravity low north of the fault that has been partially dismembered with segments of the basin scattered amongst tectonic slivers. Finally, the southernmost part of the model contains higher density pre-arc basalts and a band containing Coniacian red chert that is modelled as a somewhat lower density southward dipping layer.

Interestingly, the Malena beach geologic cross-section (Figure 4) shows a small-scale ASFZ flower structure that is replicated on a larger scale in the gravity model. In the gravity model, the Malena beach section shows up as a single higher density block, fault bounded to the north and south, by sections of lower density sedimentary basins. This is due to the spatial resolution of the gravity measurements (2–300 m), but overall the structures are similar geometry.

Discussion

In this section, we discuss the timing of deformation as inferred from mapped cross-cutting relationships; then, the structure of the Azuero Peninsula, as constrained by gravity data, local transects, regional cross-sections, and mapping. Finally, we discuss the implications of the cross-sections in the development of forearcs. This discussion is enhanced from a myriad of published geochronologic data (SM1) of the Azuero Peninsula, which we plotted in a geologic context constrained by detailed ground mapping for the first time (Figure 2). The field and gravity observations combined with published data allow meaningful comparisons and correlations to be made, while highlighting at the same time gaps in the geological understanding of the peninsula.

Timing of Deformation

Timing of deformation is well constrained in the Azuero Peninsula. Because nearly undeformed mafic dikes (39.4 ± 2.7 Ma, Tournon and Bellon 2009) cross-cut deformed sequences to the north and south of the mapped area (Figure 2), the pervasive deformation and local development of ductile fabrics, predate dike intrusion. The mafic dykes, however, do not intrude Cenozoic strata. Therefore, whole-margin pervasive deformation took place after the youngest arc activity (~50 Ma in the Azuero Peninsula, Figure 2), but before intrusion of the dikes (~39 Ma), possibly related to collision and accretion of seamounts (Hoernle *et al*. 2002; Buchs *et al*. 2011), or a more regional deformational process (Montes *et al*. 2012). Dike intrusion was then followed by emergence and erosion of the forearc, and accumulation of the Tonosi Fm. This timing of deformation was also provided by Corral et al. (2011, 2013) based on the geological mapping of the central Azuero Peninsula arc sequences.

Faulting along the ASFZ cross-cut units as young as lower Miocene (Perez-Consuegra *et al*. 2018), left-laterally separating the mapped dike swath ~17 km (Figure 2), so latest activity along the ASFZ must be younger than early Miocene. A post-early Miocene age is consistent with the kinematic changes taking place in this part of the margin at the time (Farallon Plate fission at 23 Ma, Westbrook *et al*. 1995; Lonsdale 2005; Rockwell *et al*. 2010; McGirr *et al*. 2021), but the age of first activity of the ASFZ could be as old as late Eocene.

The Suture

Based on the new geological map, the newly performed regional cross-section, and the presented

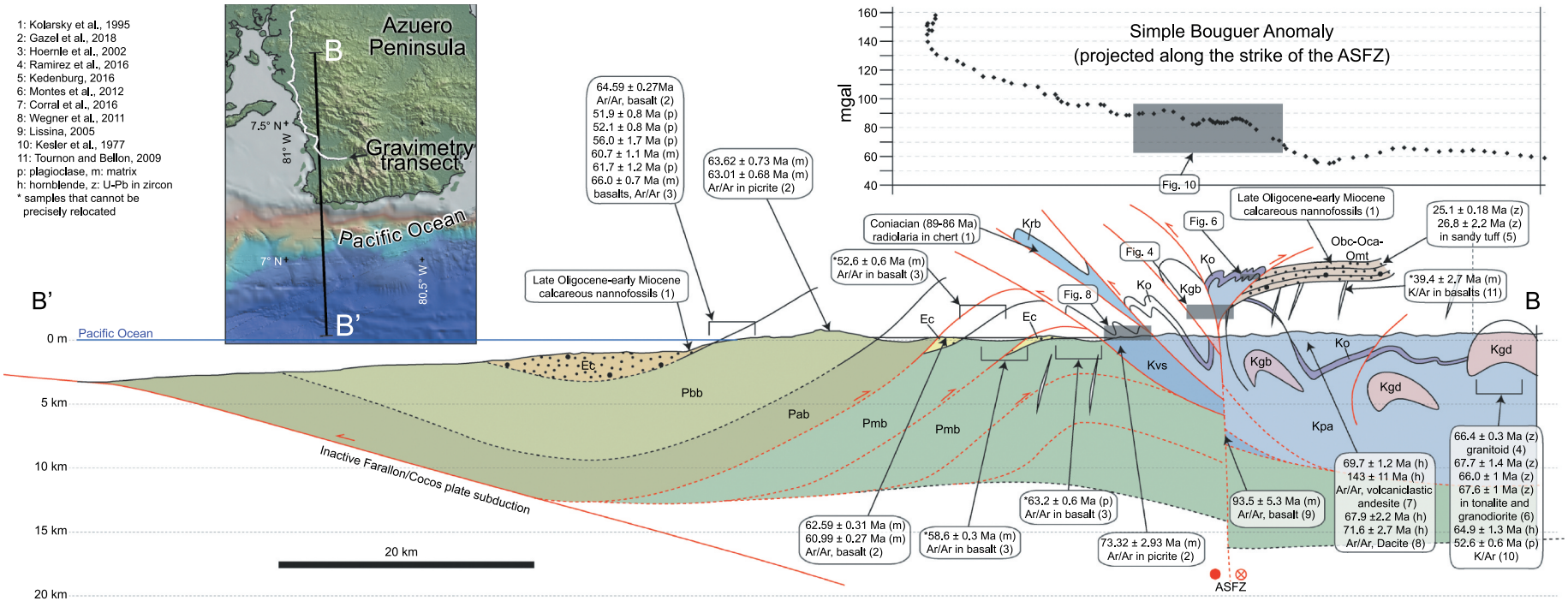

Figure 11. General cross-section along the western edge of the Azuero Peninsula. Upper left inset shows the general location of the cross-section (B-B') and of the gravimetry transect (white). Upper right inset shows the gravity profile measured along the main access road projected along the strike of the ASFZ. The position of geochronological data and thrust sheets containing forearc sequences was reconstructed using down-plunge projection.

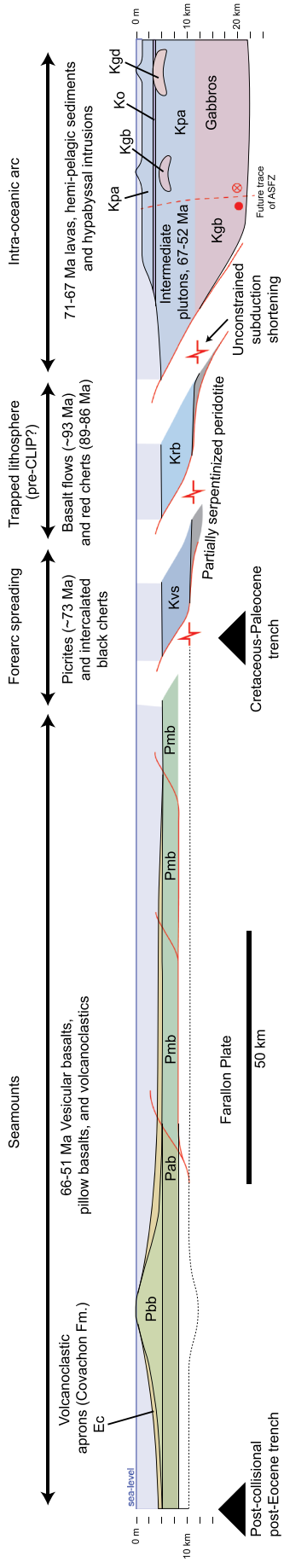

Figure 12. Reconstruction of margin geometry before the accretion of seamounts in middle Eocene times. The two south-verging crystalline thrust sheets were reconstructed assuming a simple sequence of imbricate thrusts. Their length and thicknesses were estimated from the geologic map and the general cross-section (Fig. 11). Dashed red line shows the future location of the ASFZ.

gravity profile (Figure 11), the suture between the accreted seamounts and the margin of the intra-oceanic arc cannot be coincident with the ASFZ in western Azuero (as suggested by Buchs *et al*. 2011). Instead, it must be located further south (Figure 2), consistent with palaeomagnetic declination data (Rodriguez-Parra *et al*. 2017), immediately south of the ultramafic, serpentinized peridotite sole found near Filipinas Hill (Figure 2), and the deep-marine sedimentary rocks, olivine-rich lavas, pillow basalts, and laminar basaltic flows that crop out along La Honda, Guayabo and Cañabrava creeks (Figures 2, and 7). This suture was named the Cerro Honda Fault by Rodriguez-Parra *et al*. (2017), a structure mostly covered by recent deposits along the Quebro River Valley (Figure 2). Our work additionally shows that the rock sequences found south of the ASFZ do not conform to Raymond's (1984) definition of melange, as the bodies within the shear zone are mappable, coherent, and not embedded in a fragmented matrix of finer-grained material. We therefore suggest dropping the term 'Azuero Melange' (Buchs *et al*. 2010) in western Azuero. Overall, the ASFZ gravity model shows an 8–9 km wide flower structure with kilometre-scale, radiating outward crustal thrust sheets. This structure sits at the edge of an approximately 20–30 mgal step in the regional gravity field (Figure 11), suggesting higher density crust to the south and lower density crust to the north.

Plateau

The Coniacian red chert sequence and associated basalts are located within a coherent, mappable, ~8 km long south-verging, crystalline thrust sheet sandwiched between the Central American arc sequences and the crystalline thrust sheet exposed along the La Honda, Guayabo and Cañabrava creeks (Figure 11). While the map (Figure 2) confirms its position as a discrete unit south of the ASFZ, existing biostratigraphic age determinations (89–86 Ma, Kolarsky *et al*. 1995), suggest that this unit is roughly coeval with the main ~89–90 Ma Caribbean plateau extrusion event (Sinton *et al*. 1998; Dürkefälden *et al*. 2019). However, wide-ranging geochronological determinations elsewhere in the Peninsula (from 93 to 145 Ma, Lissina 2005; Corral *et al*. 2016), suggest that these radiolarites may be capping not only CLIP basement, but also an old, complex pre-CLIP basaltic sequences, embedded within the forearc (e.g. DeBari *et al*. 1999). Crucially, this thrust sheet contains no record of hemipelagic limestone and interbedded basalt flows, typical of the younger Azuero proto-arc. While further geochronological and geochemical work would be needed to confirm the affinity of the basalts above and below the Coniacian red chert unit, trace element geochemistry also suggests plateau affinities (Buchs *et al*. 2010).

Structure of the Azuero Forearc

Inflection points along the gravity profile correspond to observed changes in lithology (Figures 2 and 11). Significant anomalies with large wavelengths may correspond to relatively shallow, low-density, ~1500 m thick Cenozoic strata (Kolarsky *et al*. 1995), and deeper, intermediate to felsic plutons (e.g. Montuoso and Valle Rico granitoids, Corral *et al*. 2011) at the northern third of the cross-section (Figure 11). Smaller wavelength changes near the ASFZ (Figure 10) may correspond to kilometre-scale tectonic wedges of contrasting densities such as slivers of Cenozoic strata, carbonates of the Ocu Formation, gabbros and basaltic sequences, like the faulted blocks exposed along Malena Beach (Figure 4). Near the centre of the gravity profile (Figure 11, inset), three step-like jumps bring anomaly values from ~85 mGal to 130 mGal, perhaps indicating denser rocks, like the peridotites exposed in the lowermost south-verging fault slice (Figure 3e-f). Further south, the observed 160 mGal anomaly may be explained by thickened, mafic crustal slices. We interpreted a north-verging crustal-scale duplex made of slices of seamounts (Pmb in Figure 11), detached and stacked above the former subduction channel, and below the suture zone (see below).

Reconstruction

The local geologic cross-sections (Figures 4, 6, 8 and 11), allow us to put forward a reconstruction by bringing the key beds to a horizontal, pre-deformational position. To the north, the hemipelagic carbonates and interbedded lava flows of the Ocu Fm. were used as key beds to reconstruct the geometry of the arc, and the down-plunge exposures afforded by the ASFZ, allowed better examination of its structure. Gravity and mapped structure was used to propose a reconstruction to the south, in the seamount domain.

Two crystalline thrust sheets above the suture were reconstructed to a pre-deformational state using the black and red cherts and interbedded lava flows as key beds. Dip data, exposed length, and folding intensity were used to estimate minimum thrust sheet lengths

and thicknesses. Once horizontal, the thrust sheets are sequentially restored south of the arc – in a forearc position – where an unconstrained amount of shortening and tectonic erosion along the subduction margin occurred (Figure 12). The bottom thrust sheet contains folded and faulted basalt flows, often picritic, and conformably interbedded chert and siliceous mudstone, with a distinctive ultramafic, serpentinized peridotite and picritic basalt sole~73 Ma (Gazel *et al*. 2018), marking the lowermost crustal levels exposed along this transect. The top thrust sheet contains a sequence of interbedded basalts and Coniacian red cherts (Kolarsky *et al*. 1995). Once restored, the two imbricated, south-verging thrust sheets may correspond to faulted and folded crustal elements originally present in the forearc at the trailing edge of the thickened plateau and its magmatic arc (Figure 12).

An imbricated forearc interpretation differs from Gazel's *et al*. (2018) interpretation of the margin's picrites as one of the oldest accreted Galapagos hotspot tracks, remarkably preserving a southern Galapagos affinity. Our observations and published age dates suggest that this sequence was built in a deep marine setting, in a forearc position, more outboard than the older fragments capped by red radiolarites, more consistent with a subduction initiation forearc crust (Whattam *et al*. 2020; Leon *et al*. 2022), than with a Galapagos-derived seamount. We prefer the former interpretation because regardless of their genesis (seamount or supra-subduction) all the lavas may have acquired a Galapagos signature, either by primary processes, or by contamination.

The structure of the accreted seamounts to the south (Hoernle *et al*. 2002; Buchs *et al*. 2011) is less certain, as bedding is crudely delineated by aligned vesicles within the otherwise massive basalts, and no pelagic or hemipelagic units exist here to track deformation. However, clastic and volcanoclastic Cenozoic strata mark the location of north-verging faults that repeat the sequence, while gravity data suggest an excess of mass that can be interpreted as thickening by repeating basaltic seamount sequences. We therefore interpreted an antiformal stack duplex (Figure 11), using the faults marked by the repeated upper clastic and volcanoclastic aprons, drawing the sheets to a depth that may explain the observed gravity anomaly. This duplex piles up the accreting seamount slices underneath the imbricated, south-verging thrust sheets.

Considering Azuero's tectonic history, the role of buoyant features colliding into the margin shaped the structure of this SSZ ophiolite. Our reconstruction (Figure 12) shows two surviving pieces of oceanic crust in a forearc position. First, picritic lavas, cherts and associated peridotites that formed in a forearc position (Kvs in Figure 12), roughly 15 Ma after the 89–90 Ma main extrusion event of the CLIP (Sinton *et al*. 1998; Dürkefälden *et al*. 2019), initiation of subduction prompted by plume activity (Whattam *et al*. 2020), and onset of arc magmatism (Leon *et al*. 2022). Second, a slice of likely older crust, probably pre-CLIP capped by Coniacian radiolarites (Kolarsky *et al*. 1995), that may be relict of crust prior to subduction initiation, and extrusion of the forearc lavas (Krb in Figure 12).

Implications

This study highlights the importance of deformation structures and crosscutting relations of SSZ ophiolites to refine tectono-magmatic models of arc-forearc settings, as geochemical arguments alone have difficulties discriminating between possible tectonic scenarios (Dickinson *et al*. 1996; Metzger *et al*. 2002). Very few studies approach the processes of deformation of SSZ ophiolite sequences in relation to accretion to the upper plate margin. In the next paragraph we briefly discuss other ophiolitic sequences where similar styles or sequences have been described.

Other ophiolites around the world, such as those in the central Asian Orogenic Belt (CAOB) in northern China, show a ~60 km wide belt of imbricated thrust faults that span an arc-ophiolite-accretionary complex, with ophiolitic melanges (Fu *et al*. 2018), glaucophane schists, mylonites and granitoids. These ophiolites, such as the Diyanmiao ophiolite (Li *et al*. 2018), have a complete section from bottom to top that includes hazburgite, gabbros (bedded and isotropic) less than 100 m thick, anorthosites, breccia and pillow basalt sequences up to 1000 m-thick, and interbedded chert. Accretion and preservation of CAOB ophiolites resulted from imbrication of thrust sheets in a Himalayan-type collision where opposite-verging active margins collided, closing an ocean basin (Xiao *et al*. 2003). Formation of some of these ophiolites followed a path similar to those proposed for the intra-oceanic Marianas forearc (Ishizuka *et al*. 2014), including a transition from forearc basalts to boninites of only 7 Ma (Li *et al*. 2020).

Tethyan ophiolites, perhaps the most studied ophiolite sequences, are obducted onto collisional continental margins as relatively intact allochthonous lithospheric slabs, containing metamorphic soles which represent relics of the MORB lithosphere underplating the SSZ ophiolites (Beccaluva *et al*. 2004; Tremblay *et al*. 2011). The structure of the Semali ophiolite is different from other Tethyan ophiolites, as it forms the uppermost tectonic nappe in an imbricated stack of oceanic rocks, resting in

a discontinuous metamorphic sole structure (Dilek and Furnes 2014). Analogous to the CAOB, and the Semali ophiolites, the structure in Azuero is dominated by imbricated thrust sheets with the same vergence as the subduction zone at the moment of accretion. Unlike the CAOB ophiolites, and the Semali ophiolite, the Azuero ophiolite is not associated with any melange sequences, high-pressure metamorphic rocks, or a thin, older metamorphic sole. Contrasting structural interpretations regarding the plume-type, subduction-unrelated, Western Colombia ophiolite (Dilek and Furnes 2014) hinder a more detailed comparison to be made with other circum-Caribbean ophiolites. For instance, Kerr *et al*. (1998), suggest that collision against the ~20-km-thick CLIP crust accreted slices of basalt, gabbro, and ultramafic rocks to the overriding plate, with the same vergence as that of the subduction zone. On the other hand, Bourgois *et al*. (1987), and Nivia (1996), suggest that the Western Colombia ophiolite is the result of obduction of a section of the CLIP, with a vergence opposite to the subduction zone. Clearly, a better understanding of the formation and emplacement mechanisms of ophiolite could be derived from more detailed studies focused on the structure of ophiolites.

Conclusions

The central portion of the western Azuero Peninsula preserves two south-verging crystalline thrust sheets that contain: 1) the record of subduction initiation in the trailing edge of the Caribbean Large Igneous Plateau (CLIP) in the form of a ~73 Ma supra-subduction zone ophiolite; and 2) a surviving piece of pre-CLIP oceanic crust. There is no record of the subduction channel in the form of melanges, high-pressure metamorphic rocks, or metamorphic soles. Collision of the Azuero margin with Galapagos-derived seamounts during middle Eocene times clogged the subduction zone, slicing the incoming seamounts into an antiformal stack that raised, and helped preserve the forearc ophiolite and the pre-CLIP crust. A mostly Oligocene clastic wedge was accumulated onto the collisional margin, and later displaced along the Azuero-Sona fault zone. This work helps fill a void in the geologic mapping of the Central American margin with detailed field mapping along creek beds and tidal wave-cut platforms with 639 field stations and a ~50 km-long gravity survey.

Acknowledgments

In memory of Henry Martinez. This research was supported by the Smithsonian Tropical Research Institute (STRI), Universidad de los Andes in Bogotá, Colombia, and PCP-PIRE program (University of Florida). The authors would like to thank all the participants of the Uniandes-Azuero Field Camp 2014-2015, who enthusiastically contributed in the mapping project, Camilo Arenas, Manuel Ariza, Aura Cuervo, Sergio Diaz, Rocio Jaimes, Paula Leal, Melanie Patiño, Nicolas Perez-Consuegra, Luis Pizano, Lina Pua, Andres Rodriguez-Corcho, Marco Rodriguez, Enrique Suarez, Edgar Tarazona, German Bayona, Jorge W. Moreno, Carlos Jaramillo, Camila Vallejo, Bruce McFadden, Agustin Cardona, Idael F. Blanco-Quintero, Fabio Ferri, and the PCP-PIRE team from the University of Florida, for their constructive observations, and help during both field, and analytical stages. Special thanks to Carlos A. Rosero for logistical support in the field. Lydian Boschman, Isaac Corral, and David Buchs are thanked for in-depth, constructive reviews.

Disclosure statement

No potential conflict of interest was reported by the authors.

Funding

The work was supported by the University of Florida PCP-PIRE Smithsonian Tropical Research Institute Universidad de los Andes [Uniandes P12. 160422.002/001].

ORCID

Carolina Ortiz-Guerrero http://orcid.org/0000-0003-1620-5230
Alejandro Cortes-Calderon http://orcid.org/0000-0002-5690-6907
Lina Perez-Angel http://orcid.org/0000-0002-2920-7967

References

Ariza-Acero, M., Spikings, R., Beltran-Triviño, A., Ulianov, A., and Von Quadt, A., 2022, Geochronological, geochemical and isotopic characterisation of the basement of the chocó-panamá block in Colombia: Lithos, v. 412-413, p 106598. 10.1016/j.lithos.2022.106598

Barat, F., Mercier de Lepinay, B., Sosson, M., Muller, C., Baumgartner, P.O., and Baumgartner-Mora, C., 2014, Transition from the farallon plate subduction to the collision between South and Central America: Geological evolution of the panama isthmus: Tectonophysics, v. 622, p 145–167. 10.1016/j.tecto.2014.03.008

Beccaluva, L., Coltorti, M., Giunta, G., and Siena, F., 2004, Tethyan vs. Cordilleran ophiolites: A reappraisal of distinctive tectono-magmatic features of supra-subduction complexes in relation to the subduction mode: Tectonophysics, v. 393, no. 1–4, p. 163–174. 10.1016/j.tecto.2004.07.034

Boschman, L.M., van Hinsbergen, D.J., and Spakman, W., 2021, Reconstructing jurassic-cretaceous intra-oceanic subduction evolution in the northwestern Panthalassa Ocean Using Ocean plate stratigraphy from Hokkaido, Japan: Tectonics, v. 40, no. 8, p. e2019TC005673. 10.1029/2019TC005673

Bourgois, J., Calle, B., Tournon, J., and Toussaint, J.-F., 1982, The andean ophiolitic megastructures on the Buga-Buenaventura transverse (Western Cordillera—Valle Colombia: Tectonophysics, v. 82, no. 3–4, p. 207–229. 10.1016/0040-1951(82)90046-4

Bourgois, J., Toussaint, J.-F., Gonzalez, H., Azema, J., Calle, B., Desmet, A., Murcia, L.A., Acevedo, A.P., Parra, E., and Tournon, J., 1987, Geological history of the cretaceous ophiolitic complexes of northwestern South America (Colombian Andes: Tectonophysics, v. 143, no. 4, p. 307–327. 10.1016/0040-1951(87)90215-0

Buchs, D.M., Arculus, R.J., Baumgartner, P.O., Baumgartner-Mora, C., and Ulianov, A., 2010, Late cretaceous arc development on the SW margin of the Caribbean Plate: Insights from the Golfito (costa rica) and Azuero (Panama) complexes: Geochemistry, Geophysics, Geosystems, v. 11, no. 7, p. 35. 10.1029/2009GC002901

Buchs, D.M., Arculus, R.J., Baumgartner, P.O., and Ulianov, A., 2011, Oceanic intraplate volcanoes exposed: Example from seamounts accreted in Panama: Geology, v. 39, no. 4, p. 335–338. 10.1130/G31703.1

Buchs, D.M., Baumgartner, P.O., Baumgartner-Mora, C., Flores, K., and Bandini, A.N., 2011, Upper Cretaceous to miocene tectonostratigraphy of the azuero area (Panama) and the discontinuous accretion and subduction erosion along the middle American margin: Tectonophysics, v. 512, no. 1–4, p. 31–46. 10.1016/j.tecto.2011.09.010

Buchs, D.M., Irving, D., Coombs, H., Miranda, R., Wang, J., Coronado, M., Arrocha, R., Lacerda, M., Goff, C., and Almengor, E., 2019, Volcanic contribution to emergence of Central Panama in the early miocene: Scientific Reports, v. 9, no. 1, p. 1–16. 10.1038/s41598-018-37790-2

Burger, H.R., Sheehan, A.F., Jones, C.H., and Burger, H.R., 2006, Introduction to applied geophysics: Exploring the shallow subsurface. New York: WW Norton.

Case, J.E., Shagam, R., and Giegengack, R.F.1990Geology of the Northern Andes; an overview. in Dengo, G., and Case, J.E. eds., The caribbean region, volume H: Boulder, CO: Geological Society of America, p. 177–200.

Coates, A.G., Collins, L.S., Aubry, M.-P., and Berggren, W.A., 2004, The geology of the Darien, Panama, and the late miocene-pliocene collision of the Panama arc with northwestern South America: Geological Society of America Bulletin, v. 116, no. 11–12, p. 1327–1344. 10.1130/B25275.1

Compton, R.R., 1985, Geology in the field": New Jersey, John Wiley & Sons

Corral, I., Cardellach, E., Corbella, M., Canals, A., Gomez-Gras, D., Griera, A., and Cosca, M.A., 2016, Cerro quema (Azuero Peninsula, Panama): Geology, alteration, mineralization, and geochronology of a volcanic dome-hosted high-sulfidation au-cu deposit: Economic Geology, v. 111, no. 2, p. 287–310. 10.2113/econgeo.111.2.287

Corral, I., Cardellach, E., Corbella, M., Canals, À., Griera, A., Gómez-Gras, D., and Johnson, C.A., 2017, Origin and evolution of mineralizing fluids and exploration of the cerro quema Au-Cu deposit (Azuero Peninsula, Panama) from a fluid inclusion and stable isotope perspective: Ore Geology Reviews, v. 80, p 947–960. 10.1016/j.oregeorev.2016.09.008

Corral, I., Giera, A., Gomez-Gras, D., Corbella, M., Canals, A., Pineda-Falconett, M., and Cardellach, E., 2011, The Geology of the Cerro Quema Au-Cu deposit (Azuero Peninsula, Panama: Geologica Acta, v. 9 no. 3–4, p. 481–498

Corral, I., Gomez-Gras, D., Griera, A., Corbella, M., and Cardellach, E., 2013, Sedimentation and volcanism in the panamanian cretaceous intra-oceanic arc and fore-arc: New insights from the Azuero peninsula (SW Panama: Bulletin de la Societe Geologique de France, v. 184, no. 1–2, p. 35–45. 10.2113/gssgfbull.184.1-2.35

D'agostino, G., Germak, A., Quagliotti, D., Pinzon, O., Batista, R., and Echevers, L., 2010, Gravity measurements in panama with the IMGC-02 transportable absolute gravimeter in Mertikas, S. ed., Gravity, geoid and earth observation: Berlin, Springer-Verlag pp. 101–105

DeBari, S.M., Taylor, B., Spencer, K., and Fujioka, K., 1999, A trapped Philippine Sea plate origin for MORB from the inner slope of the Izu–Bonin trench: Earth and Planetary Science Letters, v. 174, no. 1–2, p. 183–197. 10.1016/S0012-821X(99)00252-6

Dickinson, W.R., Hopson, C.A., and Saleeby, J., 1996, Alternate origins of the coast range ophiolite (California); introduction and implications: GSA Today: A Publication of the Geological Society of America, v. 6 no. 2, p. 1–10

Dilek, Y., 2003, Ophiolite concept and its evolution in Dilek, Y., and Newcomb, S. eds., Special papers-geological society of America, Vol. 373: Boulder, CO, Geological Society of America,pp. 1–16

Dilek, Y., and Furnes, H., 2009, Structure and geochemistry of Tethyan ophiolites and their petrogenesis in subduction rollback systems: Lithos, v. 113, no. 1–2, p. 1–20. 10.1016/j.lithos.2009.04.022

Dilek, Y., and Furnes, H., 2014, Ophiolites and their origins: Elements, v. 10, no. 2, p. 93–100. 10.2113/gselements.10.2.93

Dilek, Y., and Furnes, H., 2019, Tethyan ophiolites and Tethyan seaways: Journal of the Geological Society, v. 176, no. 5, p. 899–912. 10.1144/jgs2019-129

Di Marco, G., Baumgartner, P.O., and Channell, J.E.T., 1995, Late cretaceous-early tertiary paleomagnetic data and a revised tectonostratigraphic subdivision of costa rica and western Panama in Mann, P. ed., Geologic and tectonic development of the Caribbean plate boundary in southern Central America, Vol. 295: Boulder, Colorado, Geological Society of America,pp. 1–27

Duque-Caro, H., 1990, The choco block in the northwestern corner of South America; structural, tectonostratigraphic, and paleogeographic implications: Journal of South American Earth Sciences, v. 3, no. 1, p. 71–84. 10.1016/0895-9811(90)90019-W

Dürkefälden, A., Hoernle, K., Hauff, F., Wartho, J.-A., van den Bogaard, P., and Werner, R., 2019, Age and geochemistry of the beata ridge: Primary formation during the main phase (~89 Ma) of the caribbean large igneous province: Lithos, v. 328, p 69–87. 10.1016/j.lithos.2018.12.021

Farris, D.W., Cardona, A., Montes, C., Foster, D., and Jaramillo, C., 2017, Magmatic evolution of Panama Canal volcanic rocks: A record of arc processes and tectonic change: Plos One, v. 12, no. 5, p. e0176010. 10.1371/journal.pone.0176010

Fisher, S.P., 1965, Upper Cretaceous strata of northwestern Panama: American Association of Petroleoum Geologist Bulletin, v. 49, p 433–444. 10.1306/A6633630-16C0-11D7-8645000102C1865D

Fu, D., Huang, B., Kusky, T.M., Li, G., Wilde, S.A., Zhou, W., and Yu, Y., 2018, A middle permian ophiolitic mélange belt in the

solonker suture zone, western inner Mongolia, China: Implications for the evolution of the Paleo-Asian ocean: Tectonics, v. 37, no. 5, p. 1292–1320. 10.1029/2017TC004947

Gazel, E., Trela, J., Bizimis, M., Sobolev, A., Batanova, V., Class, C., and Jicha, B., 2018, Long-lived source heterogeneities in the galapagos mantle plume: Geochemistry: Geophysics, Geosystems, v. 19, no. 8, p. 2764–2779. 10.1029/2017GC007338

Guidice, D., and Recchi, G., 1969, Geología del area del proyecto minero de Azuero. Panama: United Nations.

Herrera, F., Manchester, S., and Jaramillo, C., 2012, Permineralized fruits from the late eocene of panama give clues of the composition of forests established early in the uplift of Central America: Review of Paleobotany and Palynology, v. 175, p 10–24. 10.1016/j.revpalbo.2012.02.007

Hershey, O.H., 1901, The geology of the central portion of the Isthmus of Panama: Bulletin of the department of geology: University of California, v. 2 no. 8, p. 231–267

Hoernle, K., Abt, D.L., Fischer, K.M., Nichols, H., Hauff, F., Abers, G.A., van den Bogaard, P., Heydolph, K., Alvarado, G., Protti, M., and Strauch, W., 2008, Arc-parallel flow in the mantle wedge beneath costa rica and Nicaragua: Nature, v. 451, no. 7182, p. 1094–1097. 10.1038/nature06550

Hoernle, K., Hauff, F., and van den Bogaard, P., 2004, 70 m. Y. history (139-69 Ma) for the Caribbean large igneous province: Geology, v. 32, no. 8, p. 697–700. 10.1130/G20574.1

Hoernle, K., van den Bogaard, P., Werner, R., Lissinna, B., Hauff, F., Alvarado, G., and Garbe-Schanberg, D., 2002, Missing history (16-71 Ma) of the Galapagos hotspot: Implications for the tectonic and biological evolution of the Americas: Geology, v. 30, no. 9, p. 795–798. 10.1130/0091-7613(2002)030<0795:MHMOTG>2.0.CO;2

Ishizuka, O., Tani, K., and Reagan, M., 2014, Izu-bonin-mariana forearc crust as a modern ophiolite analogue: Elements, v. 10, no. 2, p. 115–120. 10.2113/gselements.10.2.115

Johnson, L.E., Fryer, P., Taylor, B., Silk, M., Jones, D.L., Sliter, W.V., Itaya, T., and Ishii, T., 1991, New evidence for crustal accretion in the outer Mariana fore arc: Cretaceous radiolarian cherts and mid-ocean ridge basalt-like lavas: Geology, v. 19, no. 8, p. 811–814. 10.1130/0091-7613(1991)019<0811:NEFCAI>2.3.CO;2

Kedenburg, M., 2016, Thermochronological constraints on Cenozoic uplift and exhumation of the Azuero Peninsula, Panamá: Implications for south central american stratigraphy and tectonics [MSc: MS Thesis.

Kellogg, J.N., and Vega, V., 1995, Tectonic development of Panama, Costa Rica, and the Colombian Andes; constraints from global positioning system geodetic studies and gravity in Mann, P. ed., Special paper geological society of America, Vol. 295: Boulder, Colorado, Geological Society of America, pp. 75–90

Kerr, A.C., Marriner, G.F., Tarney, J., Nivia, A., Saunders, A.D., Thirlwall, M.F., and Sinton, C.W., 1997, Cretaceous basaltic terranes in western Colombia: Elemental, chronological and Sr-Nd isotopic constratins on petrogenesis: Journal of Petrology, v. 38, no. 6, p. 677–702. 10.1093/petroj/38.6.677

Kerr, A.C., Tarney, J., Nivia, A., Marriner, G.F., and Saunders, A.D., 1998, The internal structure of oceanic plateaus: Inferences from obducted Cretaceous terranes in western Colombia and the Caribbean: Tectonophysics, v. 292, no. 3–4, p. 173–188. 10.1016/S0040-1951(98)00067-5

Kesler, S.E., Sutter, J.F., Issigonis, M.J., Jones, L.M., and Walker, R. L., 1977, Evolution of porphyry copper mineralization in an Oceanic Island Arc: Panama: Economic Geology, v. 72, p. 1142–1153, no. 6. 10.2113/gsecongeo.72.6.1142

Kolarsky, R.A., Mann, P., and Monechi, S., 1995, Stratigraphic development of southwestern Panama as determined from integration of marine seismic data and onshore geology in Mann, P. ed., Geologic and tectonic development of the caribbean plate boundary in Southern Central America, Vol. 295: Boulder, Colorado, Geological Society of America, pp. 159–200

Krawinkel, H., Wozazek, S., Krawinkel, J., and Hellmann, W., 1999, Heavy-mineral analysis and clinopyroxene geochemistry applied to provenance analysis of lithic sandstones from the Azuero-Sona Complex (NW Panama: Sedimentary Geology, v. 124, no. 1–4, p. 149–168. 10.1016/S0037-0738(98)00125-0

Leon, S., Avellaneda-Jiménez, D.S., Monsalve, G., Bustamante, C., and Valencia, V.A., 2022, New petrochronological evidence for magmatic activity at the Central American arc at~ 100-84 Ma: International Geology Review, p. 1–15. 10.1080/00206814.2022.2129476

Lissina, B., 2005, A profile through the Central American landbridge in western Panama: 115 Ma interplay between the Galápagos hotspot and the Central American subduction zone [Ph.D. Doctoral]: Christian-Albrechts Universität, 102 p.

Li, Y., Wang, G., Santosh, M., Wang, J., Dong, P., and Li, H., 2018, Supra-subduction zone ophiolites from Inner Mongolia, North China: Implications for the tectonic history of the southeastern Central Asian Orogenic Belt: Gondwana Research, v. 59, p 126–143. 10.1016/j.gr.2018.02.018

Li, Y., Wang, G., Santosh, M., Wang, J., Dong, P., and Li, H., 2020, Subduction initiation of the SE Paleo-Asian Ocean: Evidence from a well preserved intra-oceanic forearc ophiolite fragment in central Inner Mongolia, North China: Earth and Planetary Science Letters, v. 535, p 116087. 10.1016/j.epsl.2020.116087

Lonsdale, P., 2005, Creation of the Cocos and Nazca plates by fission of the Farallon plate: Tectonophysics, v. 404, no. 3–4, p. 237–264. 10.1016/j.tecto.2005.05.011

Lonsdale, P., and Klitgord, K.D., 1978, Structure and tectonic history of the eastern Panama basin: Geological Society of America Bulletin, v. 89, no. 7, p. 981–999. 10.1130/0016-7606(1978)89<981:SATHOT>2.0.CO;2

Mann, P., and Corrigan, J., 1990, Model for late neogene deformation in Panama: Geology, v. 18, no. 6, p. 558–562. 10.1130/0091-7613(1990)018<0558:MFLNDI>2.3.CO;2

McCabe, R., 1984, Implications of paleomagnetic data on the collision related bending of island arcs: Tectonics, v. 3, no. 4, p. 409–428. 10.1029/TC003i004p00409

McGirr, R., Seton, M., and Williams, S., 2021, Kinematic and geodynamic evolution of the Isthmus of Panama region: Implications for Central American seaway closure: GSA Bulletin, v. 133, no. 3–4, p. 867–884. 10.1130/B35595.1

Metzger, E.P., Miller, R.B., and Harper, G.D., 2002, Geochemistry and tectonic setting of the ophiolitic Ingalls Complex, North Cascades, Washington: Implications for correlations of Jurassic Cordilleran ophiolites: The Journal of Geology, v. 110, no. 5, p. 543–560. 10.1086/341759

MICI, 1996, Mapa Geologico de Panama: Ministerio de Comercio e Industrias: Division de Recursos Minerales, scale, v. 1, p. 500.000

Mickus, K., 2003, Gravity constraints on the crustal structure of Central America, the Circum-Gulf of Mexico and the Caribbean: Hydrocarbon Habitats, Basin Formation, and Plate Tectonics, v. 79, p. 638–655

Montes, C., Bayona, G., Cardona, A., Buchs, D., Silva, C., Moron, S.E., Hoyos, N., Ramirez, D.A., Jaramillo, C., and Valencia, V., 2012, Arc-Continent collision and orocline formation: Closing of the Central American Seaway: Journal of Geophysical Research, v. 117, no. B4. 10.1029/2011JB008959

Montes, C., Cardona, A., McFadden, R.R., Moron, S.E., Silva, C.A., Restrepo-Moreno, S.A., Ramirez, D.A., Hoyos, N., Wilson, J., Farris, D., Bayona, G.A., Jaramillo, C.A., Valencia, V., Bryan, J., and Flores, J.A., 2012, Evidence for middle Eocene and younger emergence in Central Panama: Implications for Isthmus closure: Geological Society of America Bulletin, v. 124, no. 5–6, p. 780–799. 10.1130/B30528.1

Montes, C., and Hoyos, N., 2020, Isthmian bedrock geology: Tilted, bent, and broken in Gomez, J., and Mateus-Zabala, D. eds., The geology of Colombia, Publicaciones Geologicas Especiales.Bogota: Servicio Geologico Colombiano, v. 3, p. 451–467.

Nivia, A., 1996, The Bolivar mafic-ultramafic complex, SW Colombia: The base of an obducted oceanic plateau: Journal of South American Earth Sciences, v. 9, no. 1–2, p. 59–68. 10.1016/0895-9811(96)00027-2

Perez-Consuegra, N., Gongora, D.E., Herrera, F., Jaramillo, C., Montes, C., Cuervo-Gomez, A.M., Hendy, A., Machado, A., Cardenas, D., and Bayona, G., 2018, New records of Humiriaceae fossil fruits from the Oligocene and Early Miocene of the western Azuero Peninsula, Panama: Boletin de la Sociedad Geologica Mexicana, v. 70, no. 1, p. 223–239. 10.18268/BSGM2018v70n1a13

Pindell, J.L., and Kennan, L., 2009, Tectonic evolution of the Gulf of Mexico, Caribbean and northern South America in the mantle reference frame: An update in James, K.H., Lorente, M.A., and Pindell, J.L. eds., The origin and evolution of the Caribbean Plate, Vol. 328: London, Geological Society,pp. 1–55

Ramirez, D.A., Foster, D.A., Min, K., Montes, C., Cardona, A., and Sadove, G., 2016, Exhumation of the Panama basement complex and basins: Implications for the closure of the Central American seaway: Geochemistry: Geophysics, Geosystems, v. 17, no. 5, p. 1758–1777. 10.1002/2016GC006289

Raymond, L.A., 1984, Classification of Melanges in Raymond, L. A. ed., Melanges: Their nature, origin, and significance. Special Paper. Boulder, CO: Geological Society of America, v. 198, p. 7–20.

Redwood, S.D., 2019, The geology of the Panama-Chocó arc, Geology and Tectonics of Northwestern South America. in Cediel, F., and Shaw, R.P. eds., Switzerland: Springer, p. 901–932.

Revillon, S., Hallot, E., Arndt, N.T., Chauvel, C., and Duncan, R.A., 2000, A complex history for the Caribbean Plateau; petrology, geochemistry, and geochronology of the Beata Ridge, South Hispaniola: The Journal of Geology, v. 108, no. 6, p. 641–661. 10.1086/317953

Rockwell, T.K., Bennett, R.A., Gath, E., and Franceschi, P., 2010, Unhinging an Indenter: A new tectonic model for the internal deformation of Panama: Tectonics, v. 29, no. 4. 10.1029/2009TC002571

Rodriguez-Parra, L.A., Gaitan, C., Montes, C., Bayona, G., and Rapalini, A., 2017, Arc-seamount collision: Driver for vertical-axis rotations in Azuero, Panama: Studia Geophysica Et Geodaetica, v. 61, p. 1–20, no. 2. 10.1007/s11200-016-1173-1

Sinton, C.W., Duncan, R.A., Storey, M., Lewis, J., and Estrada, J.J., 1998, An oceanic flood basalt province within the Caribbean Plate: Earth and Planetary Science Letters, v. 155, p. 3–4, no. 3–4. 10.1016/S0012-821X(97)00214-8

Stern, R.J., Reagan, M., Ishizuka, O., Ohara, Y., and Whattam, S., 2012, To understand subduction initiation, study forearc crust: To understand forearc crust, study ophiolites: Lithosphere, v. 4, no. 6, p. 469–483. 10.1130/L183.1

Talwani, M., Worzel, J.L., and Landisman, M., 1959, Rapid gravity computations for two-dimensional bodies with application to the Mendocino submarine fracture zone: Journal of Geophysical Research, v. 64, no. 1, p. 49–59. 10.1029/JZ064i001p00049

Tournon, J., and Bellon, H., 2009, The southern Central America puzzle: Cronology and structure. A review: Revista Geológica de América Central, v. 40, p. 11–47

Tournon, J., Triboulet, C., and Azema, J., 1989, Amphibolites from Panama: Anticlockwise P-T paths from a Pre-upper Cretaceous metamorphic basement in Isthmian Central America: Journal of Metamorphic Geology, v. 7, no. 5, p. 539–546. 10.1111/j.1525-1314.1989.tb00616.x

Tremblay, A., Ruffet, G., and Bédard, J.H., 2011, Obduction of tethyan-type ophiolites—a case-study from the thetford-mines ophiolitic complex, quebec Appalachians, Canada: Lithos, v. 125, no. 1–2, p. 10–26. 10.1016/j.lithos.2011.01.003

Vannucchi, P., Fisher, D.M., and Gardner, T.W., 2007, Reply to comment by David M. Buchs and Peter O. Baumgartner on "From seamount accretion to tectonic erosion: Formation of Osa Melange and the effects of the Cocos Ridge subduction in southern Costa Rica: Tectonics, v. 26, no. 3. 10.1029/2007TC002129

Vannucchi, P., Morgan, J.P., Silver, E.A., and Kluesner, J.W., 2016, Origin and dynamics of depositionary subduction margins: Geochemistry: Geophysics, Geosystems, v. 17, no. 6, p. 1966–1974. 10.1002/2016GC006259

von Huene, R., Ranero, C.R., and Vannucchi, P., 2004, Generic model of subduction erosion: Geology, v. 32, no. 10, p. 913–916. 10.1130/G20563.1

Wallace, L., Ellis, S., and Mann, P., 2009, Collisional model for rapid fore-arc block rotations, arc curvature, and episodic back-arc rifting in subduction settings: Geochemistry, Geophysics, Geosystems, v. 10, no. 5. 10.1029/2008GC002220

Wallace, L., McCaffrey, R., Beavan, J., and Ellis, S., 2005, Rapid microplate rotations and backarc rifting at the transition between collision and subduction: Geology, v. 33, no. 11, p. 857–860. 10.1130/G21834.1

Wegner, W., Wörner, G., Harmon, M.E., and Jicha, B.R., 2011, Magmatic history and evolution of the Central American land bridge in Panama since the Cretaceous times: Geological Society of America Bulletin, v. 123, no. 3/4, p. 703–724. 10.1130/B30109.1

Westbrook, G.K., Hardy, N.C., and Heath, R.P., 1995, Structure and tectonics of the Panama-Nazca Plate boundary: Special Paper Geological Society of America, v. 295, p. 91–109

Whattam, S.A., 2018, Primitive magmas in the early Central American volcanic arc system generated by plume-induced subduction initiation: Frontiers in Earth Science, v. 6, p 18. 10.3389/feart.2018.00114

Whattam, S.A., Montes, C., and Stern, R.J., 2020, Early central American forearc follows the subduction initiation rule: Gondwana Research, v. 79, p 283–300. 10.1016/j.gr.2019.10.002

Whattam, S.A., and Stern, R.J., 2011, The 'subduction initiation rule': A key for linking ophiolites, intra-oceanic forearcs, and subduction initiation: Contributions to Mineralogy and Petrology, v. 162, no. 5, p. 1031–1045. 10.1007/s00410-011-0638-z

Woodring, W.P., 1957, Geology and description of tertiary mollusks (gastropods; trochidae to Turritellidae). Geology and paleontology of Canal Zone and adjoining parts of Panama: U S Geological Survey Professional Paper, v. 306-A, p. 145

Wörner, G., Harmon, R., and Wegner, W., 2009, Geochemical evolution of igneous rock and changing magma sources during the formation and closure of the Central American land bridge of Panama in Kay, S.M., Ramos Victor, A., and Dickinson, W.R. eds., Backbone of the Americas: shallow subduction, plateau uplift, and ridge and terrane collision, Vol. 204: Boulder, Geological Society of America,p. 34

Xiao, W., Windley, B.F., Hao, J., and Zhai, M., 2003, Accretion leading to collision and the Permian Solonker suture, Inner Mongolia, China: Termination of the central Asian orogenic belt: Tectonics, v. 22, no. 6, p. 1–20.